Glucuronidase Immobilized in Nanoparticles for Use in Site Specific Activation of Anti-Cancer Glucuronide Prodrugs

A THESIS
SUBMITTED TO THE FACULTY OF
UNIVERSITY OF MINNESOTA
BY

MITCHELL JAMES HOVERMAN

IN PARTIAL FULFILLMENT OF THE REQUIREMENTS
FOR THE DEGREE OF
MASTER OF SCIENCE

DR. MICHAEL TRAVISANO (ADVISOR)
DR. RORY P. REMMEL (CO-ADVISOR)

March 2014

Acknowledgements

I express my appreciation to my advisors, for their guidance that contributed to my scientific development.

I thank the members of my examining committee: Dr. Rory Remmel, Dr. Michael Travisano, and Dr. Alexander Khoruts.

I appreciate the skills provided to me by former research partners: Dr. Aaron Teitelbaam, Dr. Will Ratcliff, and Dr. Ford Dennison.

Dedication

This thesis is dedicated to ….all the answers to every question I've ever had.

Abstract

The site-specific treatment of cancer can reduce the toxic side effects of chemotherapy. This thesis reviews current techniques and describes a nanotechnology approach to investigate some of the obstacles in site-specific drug targeting and activation. One site-specific approach is antibody-directed enzyme prodrug therapy, ADEPT. For this strategy, a targeting antibody directed against a tumor antigen is connected to an activating enzyme. For this project, β-glucuronidase was selected as the activating enzyme and glucuronide prodrugs, of known highly potent chemotherapeutic agents, were selected as enzyme substrates. Prodrug-activating enzymes localizing exclusively at a tumor site, with tumor-specific targeting nanoparticles, minimizes the exposure of active chemotherapeutic agents. Because of the inactivity of glucuronide prodrugs, this treatment does not kill healthy cells.

This thesis reviews current techniques on glucuronide production and is a description of a β-glucuronidase immobilization in nanoparticles procedure that investigates some of the obstacles in site-specific drug activation. Chapter I is an introduction to glucuronides, the glucuronidation procedure, and enzyme immobilization. Chapter II is a description of the glucuronidation of 4-nitrophenol, epirubicin, and homoharringtonine. It begins with the synthesis of 4-nitrophenyl-glucuronide. 4-Nitrophenol is a classic substrate for glucuronidation, is easy to prepare, and was used to evaluate the conditions for glucuronide formation and cleavage with β-glucuronidase in nanoparticles. Formation of free p-nitrophenol was determined by HPLC with UV detection.

Homoharringtonine (HHT, Omacetine, Synribo™), a highly potent chemotherapy agent, was initially chosen for an anti-cancer glucuronide prodrug for activation with β-glucuronidase embedded in nanoparticles. HHT's aliphatic alcohol may be conjugated with β-D-glucuronic acid, either by chemical or biosynthetic methods, to produce the desired glucuronide. A glucuronide of Homoharringtonine has not been reported in literature and its production is of interest for researchers to pharmaceutically evaluate a new anti-cancer glucuronide prodrug. Since HHT is such a potent cancer drug, it would be of interest to compare the cleavage of HHT-glucuronide by β-glucuronidase to a well-studied compound such as epirubicin glucuronide; that has been evaluated as ADEPT stragety.

Unfortunately, synthetic methods (the Koenig-Knorr reaction, failed to produce the desired HHT-glucuronide. Consequently, experiments with β-glucuronidase entrapped-nanoparticles were conducted with p-nitrophenol glucuronide and epirubicin glucuronide. When preparations of a glucuronide of HHT fail, due to steric hindrance, epirubicin is chosen as an alternative. Epirubicin glucuronide is mostly not activated by β-glucuronidase endogenous in microbial bio-flora within humans or naturally produced β-glucuronidase within human liver and other tissues (Hasima, H.J.,et al. 1992). Lack of promiscuity in glucuronide cleavage is possible to be beneficial in retaining site-specific activation. The production of epirubicin glucuronide is catalyzed by the human enzyme UDP-Glucuronosyltransferase 2B7 (UGT 2B7), in the liver (Innocenti, F., et al 2001).

Toxic side effects of chemotherapeutic drugs are overcome with their glucuronides by

localizing activity to a target tumor site with the activating enzyme encapsulated in a nanoparticle, invivo. After biosynthesis and HPLC purification of the anti-cancer glucuronide prodrug epirubicin glucuronide, cleavage by β-Glucuronidase was tested in-vitro. A large amount of enzyme (100 U/ml of glucuronidase in 4mM phosphate buffer pH=6.8) is needed to activate the prodrug. An added benefit of protein encapsulation is to prevent proteins being recognized as foreign invivo and consequently degraded.

In Chapter III, a suitable polymer for encapsulation of glucuronidase is alginic acid cross-linked with the addition of calcium ions, displacing sodium, forming alginate nanoparticles. The materials produce nano-droplet sized emulsions and the denaturing of protein and reduction of enzyme activity is not significant (Nesamony, J., et al. 2012). Optimization of the polymerizing procedure and material concentrations produce a nanoparticle size range appropriate for protein drug delivery. Sodium alginate, polymerization by the displacement of sodium ions with cross-linking calcium ions, is effective for the entrapment of β-glucuronidase that produces active microparticles (Burgess, D. J., and S. Ponsart. 1998). The strongly polar property of alginate is a suitable environment for activity during entrapment in nanoparticles. Active glucuronidase immobilization in nanoparticles is produced and an increase in activity, over standalone β-glucuronidase, is shown in-vitro. Nanoparticle targeting strategies outlined, in Chapter IV, with the future directions sections of this paper complete the thesis.

TABLE OF CONTENTS

ABSTRACT……..iii

TABLE OF CONTENTS.....vi

LIST OF TABLES.....xi

LIST OF FIGURES…….…….……..….xii

TABLE OF ABBREVATIONS……..……xiv

CHAPTER 1 – INTRODUCTION

I. Glucuronides as Prodrugs……1

The Concept

Overlooking Epirubicin

II. Enzyme Immobilized Nanoparticles as a Prodrug Activator……5

Alginate Nanoparticles for Protein Delivery

A Targeting Strategy

III. Hypothesis and Aims…….7

CHAPTER 2 – PRODUCTION OF GLUCURONIDES

I. Glucuronidation of 4-Nitrophenol……8

Background……8

Materials and Methods……..9

Materials

Incubation Conditions

Chromatographic Analysis of Glucuronide

Production of Standard Curve

Protein Linearity of Microsomes with 100uM 4-Nitrophenol

Time Linearity of Microsomes with 100uM 4-Nitrophenol

Results and Discussion……15

II. Attempted Glucuronidation of Homoharringtonine…….19

Background……19

Materials and Methods…….21

Materials

Enzymatic Glucuronidation of HHT Incubation Conditions

Analytical Methods

Attempted Organic Synthesis of HHT Glucuronide

Results and Discussion……28

Identification of Organic Product Cephalotaxine

III. Glucuronidation of Epirubicin……...30

Background……..30

Materials and Methods……30

Materials

Incubation Conditions for Epirubicin Glucuronide

HPLC Analytical conditions

Confirmation of Epirubicin Glucuronide in-vitro

Results and Discussion……36

CHAPTER 3 – PRODUCTION OF NANOPARTICLES

I. Control of Alginate Particle Size with Emulsions……40

Background……..40

Materials and Methods……40

Materials

Production of Alginate Gel Beads

Production of Alginate Microparticles

Production of Alginate Nanoparticles

Fine tuning of Nanoparticle Synthesis and Purification

Results and Discussion……46

II. Mild Condition Protein Embedded Nanoparticle Procedure……47

Background……47

Materials and Methods…….48

Materials

Phase Inversion Temperature (PIT) Polymerization Procedure

Results and Discussion…….….50

III. Nanoparticle Protein Immobilization and Protein Characterization...54

Background……54

Materials and Methods……..54

Materials

Activity of β-Glucuronidase

Activity of Immobilized Glucuronidase Nanoparticles

Results and Discussion…….……..60

IV. Production of Bioactive Nanoparticles……...……..62

Background……..…….……..62

Materials and Methods…….…….……62

Materials

Methods of Protein Measurement

Glucuronidase Enzyme Activity after Nanoparticle Synthesis

Method of Activity Detection

Results and Discussion……64

CHAPTER 4 – FUTURE DIRECTIONS……..…70

Cancer Cell Model

Alternative HHT Considerations

Design of HHT-Glucuronide Total Synthesis

Method of Production

Results and Discussion……74

References……75

List of Tables

Table 2.1 (4-Nitrophenol standard curve response in millivolts)…….…….12

Table 2.2 (Determination of Substrate and Product Concentrations after Incubation).17

Table 2.3 (HHT Incubation Conditions)……21

Table 2.4 (Organic reagents table)……...……..24

Table 3.1 (Riverse Biuret Method of Protein Determination)……57

Table 3.2 (Analysis of Variation in Protein Concentration Determination)……..61

Table 3.3 (Activity Rates for β-Glucuronidase on 4-Nitrophenol)……65

Table 3.4 (Mircomole Rate Change and Substrate Concentration Kinetics)…….68

List of Figures

Figure 2.1 (4-Nitrophenol Glucuronidation Reaction)……9

Figure 2.2 (4-Nitrophenol Representative Chromatograph)……..11

Figure 2.3 (4-Nitrophenol and 4-Nitrophenyl Glucuronide Standard Curve of Millivolt Response to Substrate Concentration)……...12

Figure 2.4 (Plot of Para-Nitrophenyl Glucuronide vs. Total Microsomal protein)……...15

Figure 2.5 (Time Dependent Linearity of Microsomal Glucuronidation with 100uM 4-Nitrophenol)……..16

Figure 2.6 (Tri-Acetyl-Bromo-Glucuronic-Acid-Methyl-Ester Addition)……24

Figure 2.7 (Epirubicin Before Microsomal Incubation)……32

Figure 2.8 (Epirubicin After Microsomal Incubation)……..32

Figure 2.9 (Epirubicin Glucuronide Formation)……33

Figure 2.10 (Epirubicin Glucuronide Before Glucuronidase Addition)……35

Figure 2.11 (Epirubicin Glucuronide After Glucuronidase Addition)…….35

Figure 2.12 (Epirubicin Fragmentation Pattern)……..…38

Figure 2.13 (Epirubicin Glucuronide Fragmentation Pattern)…….39

Figure 3.1 (Dark Sphered Particles Image)……...52

Figure 3.2 (Brownian Motion Movement of Particles Image)……..53

Figure 3.3 (BSA Protein Calibration Chart)……..56

Figure 3.4 (Standard Curve of Protein Concentration)……..60

Figure 3.5 (Standard Curve for Micromole Rate of Change)……66

Figure 3.6 (Lineweaver-Burke Plot of Glucuronidase Activity)……67

Figure 3.7 (Hanes-Woolf Plot)……69

Figure 4.1 (Reaction Scheme for Organic Synthesis of HHT-Glucuronide)……72

Table of Abbreviations

HHT (Homoharringtonine)

IPM (Isopropylmyristate)

TRIS (Tris(hydroxymethyl)aminomethane)

UDPGA (uridine 5'-diphospho-glucuronic acid)

DOSS (Dioctyl sodium sulfonsuccinate)

YADH (Yeast Alcohol Dehydrogenase)

AOT™ (Dioctyl sodium sulfonsuccinate)

PVA (Poly Vinyl Alcohol)

CHAPTER 1 – INTRODUCTION

I. Glucuronides as Prodrugs

The Concept

Two decades ago “1992” in a Dutch lab a prodrug approach for the site-specific treatment of cancer was published by Haisma, H. J., E. Boven, M. van Muijen, J. de Jong, W. J. van der Vijgh, and H. M. Pinedo. The title “A Monoclonal Antibody-β-Glucuronidase Conjugate as Activator of the Prodrug Epirubicin-Glucuronide for the Specific Treatment of Cancer” had the key concept that this thesis is based on. The glucuronide of an anti-cancer drug would reduce the toxicity of chemotherapy, utilizing site-specific activation. Epirubicin-glucuronide was chosen because of its stability and low cytotoxicity. When exposed to cancer cell lines A2780, MCF-7, and OVCAR-3; the cytotoxicity of epirubicin-glucuronide was at least 100 times less toxic than the parent drug epirubicin (Haisma, H., et al. 1992). This was attributed to reduced cellular uptake of the prodrug with (2.7 pmol/10^-6 cells/min) compared to the parent compound with (25 pmol/10^6 cells/min). Furthermore, epirubicin glucuronide was so stable in human blood and in cultured cancer cell lines that it was not converted into epirubicin, despite the presence of intracellular β-glucuronidase (Hasima, H,. et al. 1992). The new problem was to find a way to increase activation and cellular uptake in-vivo at the target site.

This finding was critical to the fundamental principles of site-specific activation. If a glucuronide prodrug was activated by human glucuronidase in the liver and other tissues, the tumor site-specific activation would not be so specific. They used β-glucuronidase from E.*coli* in a monoclonal antibody-enzyme conjugate that was able to activate the stable non-toxic prodrug epirubicin glucuronide at the tumor cell level. One problem with the use of bacterial glucuronidase was an immunogenic response to foreign proteins. Modifying human glucuronidase is one way this could be overcome. Another approach is to entrap copious amounts of bacterial glucuronidase within a porous, substrate diffusible, nanoparticle. The linking of one antibody to one enzyme, in this treatment, is limiting by the size of the activating area. A nanoparticle could act as a web of activity, providing a net for capturing and activating a prodrug that would result in smaller dosages and fewer side effects. (Hasima, H,. et al. 1992. "A Monoclonal Antibody-Beta-Glucuronidase Conjugate as Activator of the Prodrug Epirubicin-Glucuronide for Specific Treatment of Cancer.") The effectiveness of this chemotherapy treatment may be greatly increased by immobilizing many β-glucuronidase enzymes to each nanoparticle.

Overlooking Epirubicin

Work by Pinedo and Haisma went in a direction away from epirubicin-glucuronide due to relatively slow cleavage rates. Other anthracycline-based glucuronides were cleaved at faster rates, namely doxorubicin. Over many years, they teamed up with Boven and Graff to enhance the activation by inserting various spacer molecules between doxorubicin and glucuronic acid to produce synthetic glucuronide prodrugs that were more efficiently hydrolyzed. DOX-mGA3 was the best and resulted in a 2.7 fold higher concentration of Doxorubicin in tumor tissue than DOX-GA3 (de Graff, M., et al. 2004). Although an improvement in activation, this ease of activation results in non-specific activation at non-cancerous β-glucuronidase secreting cells.

At the time, the most feasible way to improve glucuronide prodrug therapy was to

enhance cleavage and activation. Presently, with the use of nanotechnology, activation can be achieved by significantly increasing the amount of enzyme and the proximity of activation around the tumor, assuming that the prodrug will eventually be activated if it comes in contact with an antibody-targeted nanoparticle containing glucuronidase within it. In the past, epirubicin-glucuronide was explored and its low activation efficiency was found to be less desirable compared to other more easily cleavable anthracycline glucuronide prodrugs. This harder-to-activate prodrug would be ideal for site-specific activation by an embedded protected enzyme. The most important benefit is that epirubicin-glucuronide would also be less likely to be activated in non-cancerous tissues, reducing cardiotoxicity and other non-specific side effects. The issue now was weather the activation of the prodrug could be induced by targeting active glucuronidase to the tumor site.

II. Enzyme Immobilized Nanoparticles as a Prodrug Activator

Alginate Nanoparticles for Protein Delivery

A nanoparticle is a bead-like, porous polymer with a diameter in the nanometer range. The size makes them useful for therapeutic drug and protein delivery. After researching numerous materials for drug and protein delivery, alginate was chosen as a suitable material for the encapsulated immobilization of β-glucuronidase. Because glucuronidase can activate a multitude of glucuronide-based prodrugs; β-Glucuronidase embedded nanoparticles, as prodrug activators, have enormous potential for site directed prodrug

therapy.

The process of forming alginate nanoparticles relies on calcium ion induced cross-linking of alginic acid to form a lattice like structure around the material to be entrapped. A Water-in-oil emulsion technique was employed to produce the nano-droplet sized emulsions, called nanoemulsions. This occurs when the hydrophilic alginic acid and enzyme are mixed in a hydrophobic oil base to produce “bubbles” of the material to be polymerized. This sizing of particles, through nanoemulsions, is what results in nanoparticles of the corresponding diameter, based on the size of the “bubbles”. The oil phase, in the production of alginate nanoparticles, was chosen to be isopropyl myristate (IPM) along with an emulsifying agent of dioctyl sulfosuccinate sodium salt (DOSS). This idea came from a publication showing that entrapment of BSA protein in alginate nanoparticles, with DOSS-IPM, did not significantly degrade the protein (Nesamony, J., et al 2012).

Alginate nanoparticles had previously been produced and loaded with another anthracycline named doxorubicin (Zhang, C., et al. 2011). This publication used a common EDC+NHS covalent binding method to bind a tumor-specific ligand for directing a nanoparticle to the target cancer site. The alginate was compatible with an anthracycline and allowed diffusion into and out of the particles. The production of the particles was performed followed by ligand attachment and then chemotherapeutic

anthracycline was loaded through dialysis and freeze drying. Once these robust nanoparticles are formed, they can be bonded with a multitude of ligands and loaded with a wide variety of drugs. This is contingent on material compatibility.

III. Hypothesis and Aims

The goal of this research was to develop a method that could produce enzyme-embedded nanoparticles, for site-specific anticancer prodrug activation. It may be possible to make nanodroplet sized emulsions, in the presence of a prodrug-activating enzyme, resulting in enzymatically active nanoparticles; under non-denaturing conditions without enzyme inhibiting materials and solvents.

The two most common ways to add site-specific targeting to nanoparticles involves antibodies raised against an organ-specific receptor or using a tumor-selective antigen as the target. With these objectives in mind, a nanoparticle-based approach to chemotherapy could overcome many obstacles in the treatment of cancer, because local tumor concentrations of the activated drug moiety would be enhanced. A glucuronide prodrug (inactive) would be expected to have minimal off-target side effects.

The first goal was to research a suitable prodrug that could be converted to an active form, in the presence of an activating enzyme, for cancer treatment. One intriguing possibility was found in a pharmacological review titled “Enzyme-Catalyzed Activation of Anticancer Prodrugs” (Rooseboom, M., et al.). Page 83 of this review describes activation of a glucuronide-based prodrug by an E.*coli* β-glucuronidase enzyme (EC 3.2.1.31). This review also states glucuronidated anthracycline type “prodrugs were developed to improve bioavailability and overcome the dose related cardiotoxicity of anthracyclines”.

The second goal was to develop enzyme-embedded nanoparticles. A common route to the production of nanoparticles is to produce nanoemulsions with use of an emulsifier such as a surfactant. The general technique utilized was described as a water-in-oil nanoemulsion for the preparation of calcium alginate nanoparticles (Machado, A., et al. 2012). Adaption of this procedure for our project was done with IPM as an enzyme-compatible solvent, which allows for the phase inversion temperature method to be used as a way to produce nanoparticles under mild non-denaturing conditions. The analogous property of water allows it to expand just before its freezing point to allow an appropriate sized pocket for the formation of aqueous nanoparticles. An added benefit was that these refrigeration temperatures (2-6°C) were likely to preserve the activity of the enzyme during polymerization.

Goal three was to develop a targeting method for directing the nanoparticles to a target tumor site. Various site-specific ligand and antibody conjugation concepts were referenced and considered. Although none were put into practice, some possibilities were identified.

CHAPTER 2: PRODUCTION of GLUCURONIDES

I. Glucuronidation of 4-Nitrophenol

Background

4-nitrophenol was used to determine the activity of glucuronide-forming enzymes, UDP-glucuronsyltransferase (or UGT's) within pig liver microsomes. Liver microsomes, a preperation of the endoplasmic reticulum obtained by differential centrifugation, are rich with a variety of drug metabolizing enzymes. UGT's are the glucuronide transferring enzymes in the process known as glucuronidation (Remmel 2008). Pig liver microsomes were used to gain familiarity with the process of glucuronidation, in bio-organic synthesis. To determine the conditions required for a successful incubation, a 40 minute invitro microsomal incubation was performed in the presence of 1mM UDPGA.

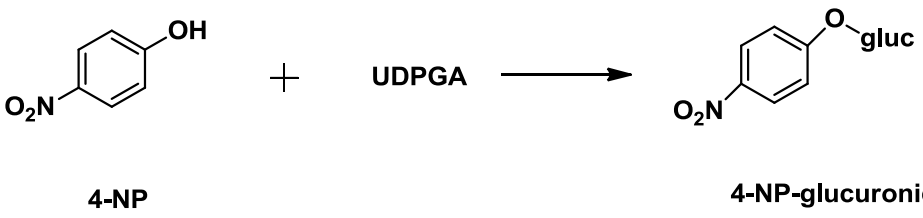

Figure 2.1 (4-Nitrophenol Glucuronidation Reaction)

Materials and Methods

Materials

Pig liver microsomes were obtained from the Remmel lab, UDPGA was ordered from SIGMA, as were Alamethicn, 4-Nitrophenol, TRIS hydrochloride and TRIS base from Malinckrodt, and Magnesium chloride from Malinckrodt (St. Louis, Mo).

Incubation Conditions

Every incubation mixture was in a total volume of 250µL. Typical conditions were made with concentrations from 5x stocks of all ingredients. In each 1.5mL test tube; 50µL of 5mM UDPGA, 50µL of 250mM TRIS buffer (pH=7.4 at 37°C), 50µL of 0.5mg/mL microsomal protein, 50µL of 25mM $MgCl_2$, 45µL of substrate, and 5µL of Alamethicin

(20μg/mL). Alamethicin, a pore forming antibiotic is added to the microsomes to allow penetration of UDPGA into the lumen of the ER (UGT active site is on the inner face of the ER membrane). Protein or time was varied in subsequent experiments.

Chromatographic Analysis of Glucuronide

Following the incubation, the 250μL reaction mixtures were quenched with 250μL of ice cold acetonitrile and placed in an ice bath for 20 minutes. Then the 1.5mL test tubes (containing 500μL volume) were centrifuged at 13,000 g for 5 minutes, to remove precipitated protein. The top 250μL was placed in an autosampler vial and run as a sequence on the Agilent 1100 HPLC.

Chromatographic conditions of the 4-nitrophenol glucuronidation assay were optimized on an Agilent Zorbax SB-C8 4.6x250mm, 5micron column (Santa Clara, CA). The separation conditions were an isocratic elution with a 50/50 mix of acetonitrile and DI H_2O at pH=6.7 with a flow rate of 1.1ml/min. A Shimadzu UV detector set at wavelength of 290nm detected 4-Nitrophenol at 3.78 minutes and its glucuronide at 1.74 minutes.

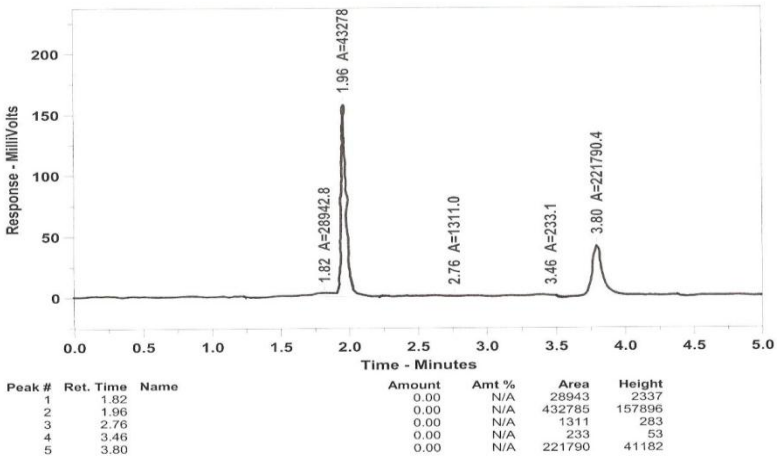

Peak #	Ret. Time	Name	Amount	Amt %	Area	Height
1	1.82		0.00	N/A	28943	2337
2	1.96		0.00	N/A	432785	157896
3	2.76		0.00	N/A	1311	283
4	3.46		0.00	N/A	233	53
5	3.80		0.00	N/A	221790	41182

Figure 2.2 (4-Nitrophenol Representative Chromatograph)

(Peak one is the more polar glucuronide and the second peak is 4-nitrophenol. In reverse phase chromatography, polar molecules elute first.)

4-Nitrophenol Standard Curve

The chromatographic conditions were used to produce a standard curve for measuring glucuronide formation in the protein linearity and time dependence experiments.

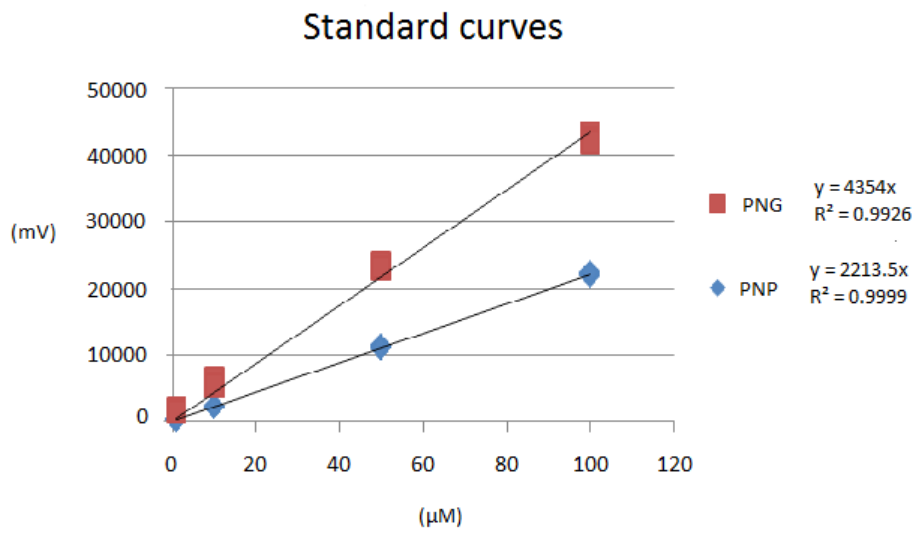

Figure 2.3 (4-Nitrophenol and 4-Nitrophenyl Glucuronide Standard Curve of Millivolt Response to micromole Substrate Concentration)

These conditions yielded over a 99% correlation coefficient when run in triplicate. The concentration of glucuronide formed can now be accurately quantified.

Table 2.1 (4-Nitrophenol standard curve response in millivolts)

PNP (uM)	mV #1	mV #2	mV #3
100	221790	219593	222768
50	111878	109946	110234
10	21374	22045	21849
1	2423	2384	2281

PNP (uM)	S.D.	C.V.	AVG
100	1626.03	0.73	221384
50	1042.30	0.94	110686
10	345.03	1.59	21756

1	73.36	3.10	2362

PNG (uM)	mV	mV	mV
100	432785	424664	420380
50	238744	230302	231266
10	64565	54988	54664
1	18518	17527	15924

PNG (uM)	S.D.	C.V.	AVG
100	6300.63	1.48	425943
50	4620.92	1.98	233437
10	5625.15	9.69	58072
1	1308.98	7.56	17323

Protein Linearity of Microsomes with 100uM 4-Nitrophenol

In a protein linearity experiment; protein concentrations of 0.05mg/mL, 0.1mg/mL, 0.25mg/mL, and 0.5mg/ml were incubated for 10 minutes at 37 degrees celsius with a starting 4-nitrophenol concentration of 100µM.

Every incubation mixture was in a total volume of 250µL, Conditions were made with concentrations from 5x stocks of all ingredients. In each 1.5mL test tube; 50µL of 5mM UDPGA, 50µL of 250mM TRIS, 50µL of a 5x stock in mg/mL of microsomal protein, 50µL of 25mM MgCl2, 45µL of substrate, and 5µL of Alamethicn (20µg/mL). 4-Nitrophenol Glucuronide was measured by UV absorbance at 290nM wavelength. The formation was calculated in micromolar concentrations, determined from the standard curve absorbance.

Time Linearity of Microsomes with 100uM 4-Nitrophenol

In linearity vs. time experiment 0.1mg/mL of protein was incubated, with 100μM 4-Nitrophenol, for times of 5, 10, 15, and 30 minutes.

Every incubation mixture was in a total volume of 250μL, Conditions were made with concentrations from 5x stocks of all ingredients. In each 1.5mL test tube; 50μL of 5mM UDPGA, 50μL of 250mM TRIS, 50μL of 0.1mg/mL microsomal protein, 50μL of 25mM $MgCl_2$, 45μL of substrate, and 5μL of alamethicin (1mg/ml stock) concentration (20μg/mL incubation concentration).

Results and Discussion

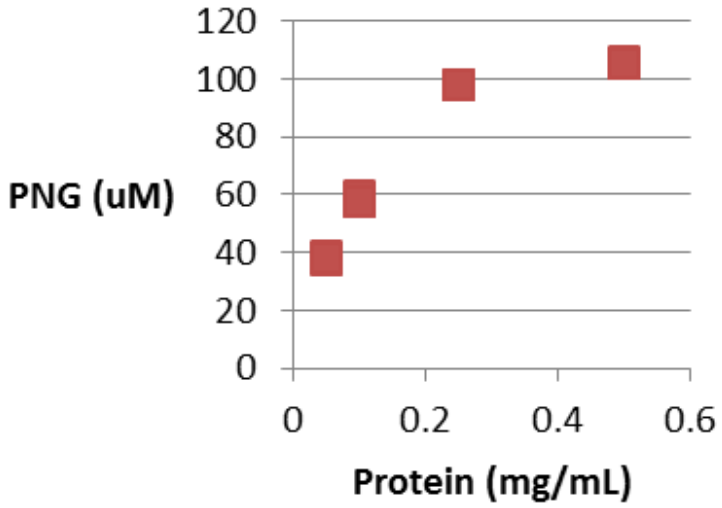

Figure 2.4 (Plot of Para-Nitrophenyl Glucuronide vs. Total Microsomal protein)

The figure (2.3) shows linearity with Glucuronidation of 100µM 4-Nitrophenol, at less than 0.1 mg/ml concentration of microsomal protein.

Concentrations that maintain a constant metabolic turnover rate will indicate a linear range of protein suitable for metabolic turnover assays. Because the metabolizing enzymes are degraded during the incubation, the rate of turnover must be kept constant with the decreasing amounts of active enzyme. The slope or rate of turnover appears to remain constant at concentrations less than 0.1 mg/ml of microsomal protein.

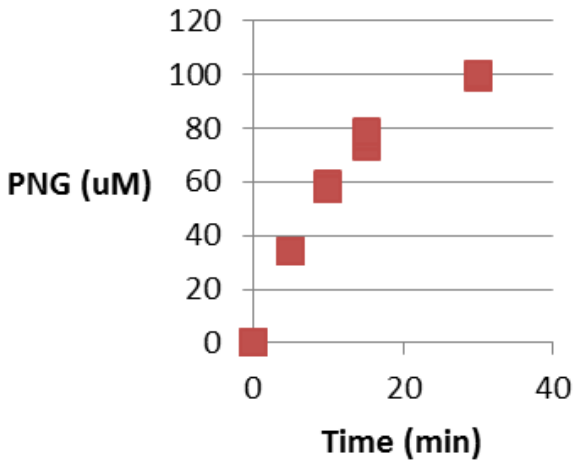

Figure 2.5 (Time Dependent Linearity of Microsomal Glucuronidation with 100µM 4-Nitrophenol)

The linearity with time experiment showed repeated success in finding glucuronide forming incubation conditions. The linearity with glucuronidation of 100µM 4-Nitrophenol occurs, within the first 10 minutes of incubation.

These required concentration of 0.1 mg/ml of microsomal protein and incubation times of less than ten minutes were determined to be the constraints required for metabolic assays involving the glucuronidation of 4-nitrophenol.

Table 2.2 (Determination of Substrate and Product Concentrations after Incubation)

Time (min)	PNG formed (μM) #1	#2	#3
0	0	0	0
5	33.95	34.33	34.43
10	59.45	57.64	57.52
15	73.03	76.72	78.73
30	98.72	99.77	100.32

Time (min)	PNG (AVG)	S.D.	C.V.
0	0	0	0
5	34.24	0.2532	0.7397
10	58.20	1.081	1.858
15	76.16	2.891	3.796
30	99.60	0.8129	0.8162

The coefficient of variation was held below 5%, for all timepoints. Following the linearity experiments of 4-nitrophenol, the potent anti-cancer drug Homoharringtonine (HHT) was obtained. Attempts to glucuronidate this drug, using the 4-nitrophenol-incubation environment, became a priority for this project.

CHAPTER 2: PRODUCTION of GLUCURONIDES

II. Attempted Production of HHT Glucuronide

Background

The drug HHT, also known as homoharringtonine, was chosen as a candidate for pro-drug design because of its potent antitumor activity. (Hook, F., et al.). Glucuronidation is a common metabolic route for the detoxification and elimination of many xenobiotics. The production of a HHT Glucuronide had not been previously reported. An attempt of its synthesis was tried enzymatically and through organic synthesis.

The synthetic route is typically more difficult and time consuming. If there are chances of letting the enzymes do all the work, it will likely have a higher product percentage yield while saving time. A direct line infusion on a thermo LC/MS/MS SRM mode for HHT-glucuronide [M+H]+=722 with fragmentation to HHT [M+H]+=546 of the extracted incubation metabolites will be used, as an assay, to look for even trace amounts of the HHT glucuronide.

An enzymatic approach to the glucuronidation of HHT was carried out following a modified procedure from (Bioconjugate Chem. 2011, 22, 753-758 by Fan and Kharasch). This procedure was improved by using human liver microsomes (donated from the Tracy lab). Human liver microsomes are known to contain the greatest variety of UGT's that can glucuronidate the greatest variety of xenobiotics. Therefore, these microsomes can offer the greatest chance for the successful glucuronidation of HHT. The enzymatic synthesis of HHT-β-D-glucuronic-acid was performed with variations of the 4-nitrophenol glucuronidation procedure. A 100mM stock solution of HHT in DMSO was used to make a 0.1% concentration of DMSO in the incubation. This 100mM stock was the maximum amount soluble in DMSO and the diluted 100μM incubation concentration was the maximum concentration possible for an uninhibited incubation (0.1% DMSO).

The organic synthesis of HHT-β-D-Glucuronic-Acid was performed in three major steps. First, the addition of triacetylbromoglucuronic acid methyl ester to Homoharringtonine (HHT) was to be accomplished with silver carbonate as a catalyst. Second, the cleavage of the three-acetyl groups from the sugar moiety was time course tested with strong base. Third, removal of the methyl ester by hydride addition with product monitoring resulted in the loss of one or two acetyl groups. This procedure could also produce combinations of these three intermediate products in varying amounts.

Materials and Methods

Materials

Human liver microsomes were obtained from the Tracy lab, UDPGA was ordered from SIGMA, Alamethicn from SIGMA, Homoharringtonine from The Chinese Academy of Sciences, TRIS hydrochloride and TRIS base from SIGMA, Magnesium chloride from Malinckrodt, and Saccharic acid 1,4-lactone monohydrate from Fluka.

Enzymatic Glucuronidation of HHT Incubation Conditions

All ingredients used for the enzymatic reaction were prepared in 5x stocks. The total volume for the reaction mixture was 500µL in a 13mm x 100mm glass test tube. The total volume was 534µL after addition of the microsomes and 50 µg of Alamethacin per milligram protein. First, 100µL of TRIS and 100µL of $MgCl_2$ were added to the 13mm x 100mm test tube. Four identical test tubes were placed in an ice bath with 17µL each of the Alamethacin (1mg/ml) and HLM protein (29.6 mg/ml) for 30min. The Alamethacin creates pores in the HLM to increase the accessibility of UDPGA for the UGT's for acting on the substrate. Next, the four test tubes were moved to a 37°C water bath followed by the addition of 100µL of each remaining ingredient. The lactone preventing glucuronidase activity, the substrate HHT, and last UDPGA was added to initiate the reaction. The four samples were incubated for one hour and then the reaction was quenched with 500µL of ice-cold acetonitrile. Then the samples were placed in an ice bath for 30 minutes to allow the protein and salt to precipitate. Finally, the samples were

placed in 1.5ml flip cap tubes and centrifuged at 13,000 RCF for 5 minutes. The supernatant was saved in the freezer and an aliquot was loaded into an auto sampler vial for HPLC analysis. Table 2.4 lists the incubation conditions.

Table 2.3 (HHT Incubation Conditions)

HLM incubation ingredients	100µL of each 5x was used		
ingredients	5x conc.	1x conc.	
TRIS buffer pH=7.4	250mM	50mM	
Saccharic acid 1,4- lactone	25mM	5mM	
MgCl	25mM	5mM	
UDPGA	5mM	1mM	
HHT	500µM	100µM	
HLM protein 1mg/ml final conc.	17µL (of 29.6mg/ml) added to the 500µL incubation		
Alamethacin 17ug/ml final conc.	17µL (of 1mg/ml) added to the 500µL incubation		

Analytical Methods for Enzymatic Incubation

Direct line infusion into a Thermo quantum LC/MS/MS triple quadrapole mass spectrometer was used with Selective Reaction Monitoring to try and identify the transition of [M+H]+=722.6 with a 176 amu loss of glucuronide to [M+H]+=546.6 HHT. The positive mode electrospray ionization tandem mass spectrum failed to detect a MW=722 ion. HPLC fluorescence was also used for a separation of possible products approach, leading to molecule identification.

An aqueous mobile phase of ammonium acetate and its conjugate base of acetic acid were prepared to a concentration of 25mM and mixed to provide a pH=4.7. Stationary phase used was methanol. These were run with a flow rate of 700µL/min in an isocratic method containing 65% MeOH, and pressure was 150bar. Separation was optimized on a Synergi Hydro reverse phase 80A measuring 250mm x 4.6mm, 4 micron. The detection was monitored with fluorescence at 280nm excitation and 320nm emission.

Attempted Organic Synthesis of HHT Glucuronide Procedure

Following the procedure from (JOC v.69 #4,2004), the Koenigs-Knorr reaction was to be used as a method for the production of HHT glucuronide. The first step of this reaction uses $AgCO_3$ as a catalyst to add the acetyl protected bromo sugar to the HHT substrate. This first step is illustrated below.

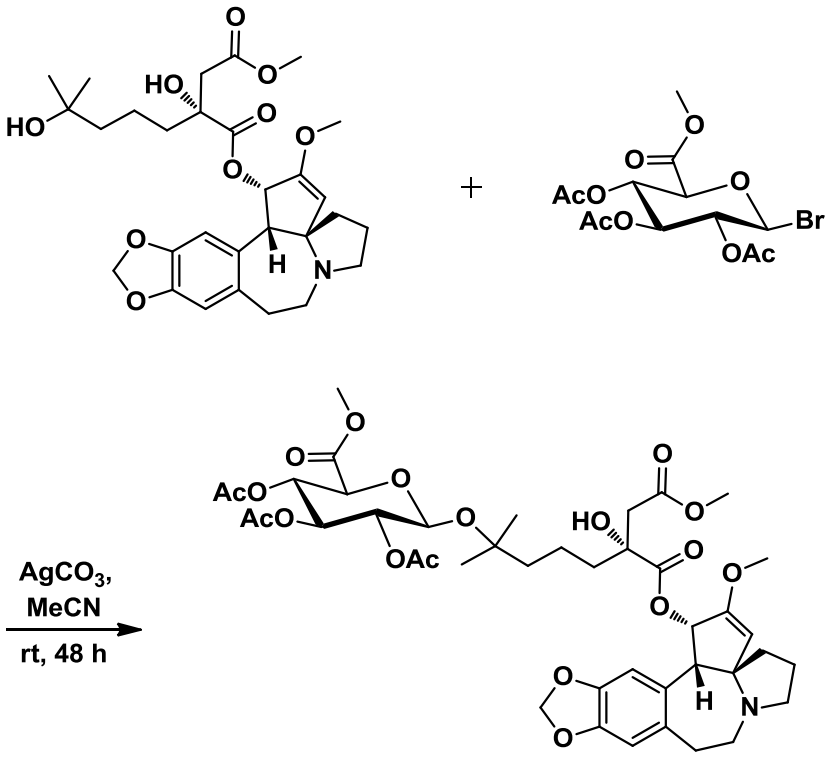

Chemical Formula: $C_{42}H_{55}NO_{18}$

Exact Mass: 861.34

Molecular Weight: 861.88

m/z: 861.34 (100.0%), 862.35 (46.7%), 863.35 (14.4%), 864.35 (3.3%)

Elemental Analysis: C, 58.53; H, 6.43; N, 1.63; O, 33.41

Figure 2.6 (Tri-Acetyl-Bromo-Glucuronic-Acid-Methyl-Ester Addition)

Silver carbonate (0.25mmols) was added to 0.12mmol of HHT in a 0.1eq (0.12mmol / 0.1eq = 1.2ml) of acetonitrile as a reaction solvent. The calculated concentrations for this first reaction are listed below in table 2.5.

Table 2.4 (Organic reagents table)

	HHT	AgCO3	Bromo sugar	Product expected
MW	545.62	275.74	397.17	861.88
Equivalents	1	2	3	1
mmols	0.12	0.25	0.36	0.12
Amount(mg)	68	69	147	107

In a 10ml round bottom reaction vessel, containing 1.2ml of acetonitrile, 70mg of silver

carbonate were dissolved with rapid stirring. 70mg of HHT was then added to the silver carbonate/acetonitrile solution followed by 150mg of Aceto Bromo Glucuronic Acid Methyl Ester. While stirring at room temperature, the solution was brought to equilibrium over 48 hours until the green crystalline slurry turned to a dark mucky brown.

The solution was poured into a filter funnel and vacuum filtered into a 50ml round bottom, washing with about 25ml of ethyl acetate. This removed the mostly insoluble silver catalyst from the solution, leaving a golden liquid. The golden reaction liquid was evaporated to dryness for 15 minutes on a Buchi rotary-evaporator, producing dark brown oil.

Analytical Method for Organic Products (Normal Phase Chromatography)

Normal phase conditions on silica TLC plates for analytical product separation were as follows. The oil-like product of this reaction was checked for reaction products by thin layer chromatography plating. The TLC plates were glass backed and silica coated and monitored under a broad UV spectrum. A spot of the reaction material was run with a spot of the starting material HHT and a spot of the bromo sugar. The conditions for separating the HHT from the reaction products were found to be 9 parts methylene chloride to 1 part methanol. These same conditions were used to separate products from starting material on a normal phase 25/40 size flash column filled with silica (4 angstrom in size). 24 test tubes containing about 10ml of solvent were collected.

Spot plating revealed two distinct spots with retention factors of Rf=0.3 and Rf=0.7. There was also a rich color running with the solvent line. The Rf=0.3 spot was identified as the starting material HHT, by co-spotting and comparison to a stock standard. The Rf=0.7 spot was to be identified by isolation of the material in the flash column.

The flash column produced 24 fractions. The first 5 were clear, containing only solvent. Fractions 6-9 containing a rich yellow color, presumed to be the Rf=0.7 spot by TLC, were pooled for further analysis. Fractions 10 and 11 got clearer and showed no spot on TLC. Fractions 12-15 showed no spot by TLC, but were very reddish-yellow and were saved for further analysis by HPLC/Fluorescence. Fractions 17-22 were a light yellow and showed a spot by TLC that compared to the starting material HHT. Fractions 23-24 were clear and showed no TLC spot, assuming only solvent was found and all organic material was previously eluted from the column.

Fractions 12-15 were reddish-yellow and of much concern, because of the richness of the color, and were analyzed by HPLC/Fluorescence. Further steps to characterize the three isolated pools, separated from the initial reaction mixture, were investigated by reverse phase liquid chromatography. Also, steps to recover the unreacted HHT from the pool of fractions 6-9 were employed.

Analytical Method (Reverse Phase Chromatography)

In the previous section, the 1st reaction step in the production of HHT glucuronide, normal phase flash column chromatography was used to produce fractions for the purification of possible reaction products. Combining three different ranges of fractions, three different pools were made. The first pool (fractions 6-9) showed a product spot on TLC where Rf=0.7. The second pool (fractions 12-15) showed no spot on TLC, but had a very rich reddish yellow color indicating the yellow HHT starting material may be present as an analog. The rotovaped second pool also produced red crystals. The third pool (fractions 17-22) showed a TLC spot with retention Rf=0.3 that compared to the starting material HHT. The presence of yellow material in pool two, along with the red crystals, encouraged the development of an analytical method, by HPLC/fluorescence, to confirm the presence or absence of a previously undetected HHT analog.

The pooled fractions were evaporated to dryness in a Buchi rotary evaporator and each fraction was dissolved in approximately 10ml of methanol. One drop (20μl), from each pool, was dissolved in an auto sampler vial containing approximately 2mL of methanol (a 1:100 dilution). 10μL of each sample were injected onto an Agilent 1100 series HPLC. The method utilized fluorescence detection with an excitation at 280nm (the optimized wavelength for HHT) and emission at 320nm. Two distinct peaks were separated with retention times of 4.05min and 5.12min. The column had a void time of 2.35min, so these

compounds were adequately retained.

An aqueous mobile phase of ammonium acetate and its conjugate base of acetic acid were prepared to a concentration of 25mM and mixed to provide a pH=4.7. Methanol was used as the organic modifier. These solvents were run at a flow rate of 700μL/min in an isocratic method at a ratio of 35:65 (65% MeOH), the column pressure was 150bar. Separation was optimized on a Synergi Hydro reverse phase 80A column measuring 250mm x 4.6mm, 4 micron (Phenomenex® Torrance, CA). The detection was monitored with fluorescence at 280nm excitation and 320nm emission.

Results and Discussion of Identification of Organic Product Cephalotaxine

The peak with retention time of 4.05min was identified as the starting material HHT. The third pool was now confirmed to be pure HHT recovered from the reaction. The second pool contained approximately a 50/50 mix of unreacted HHT and the unidentified peak at 5.12min. The first pool contained at least 95% of the 5.12min unidentified peak.

The 5.12min peak was collected to determine its mass. A mass of 743 was the most abundant and likely a decomposition product. My target mass of 863.9 was not seen, although the vast majority of unreacted HHT was recovered. The 4.05 minute peak had a mass of 316 and was identified as Cephalotaxine. This product resulted from cleavage of

the ester side chain of Homoharringtonine.

The silver carbonate catalyzed Glucuronidation in acetonitrile failed to produce the desired product. Trace amounts of moisture may have contributed to an unsuccessful reaction. This can be compensated for with 4A molecular sieves, drying the glass, reacting under argon, and using an alternative dry solvent. This is outlined in (Bioconjugate Chem. 2011, 22, 753-758 by Fan and Kharasch) as “removal of any water produced is critical for the coupling reaction”.

The same paper also outlines an enzymatic method of glucuronide production with three additional improvements over the method developed with 4-Nitrophenol. First, use saccharic acid lactone as a glucuronidase inhibitor because UGT enzymes from liver preparations naturally contain beta-glucuronidase. This would cause the enzymatic reaction to run in a futile cycle, if the UGT’s have poor activity with the substrate, glucuronidase may outcompete it. Second, aminobenzotriazole was added as a p450 inhibitor. This will reduce or eliminate any competing metabolic pathways that are not UGT’s. Third, was the use of a NADPH generating system consisting of NADP+, glucose-6-phosphate, and glucose-6-phosphate dehydrogenase. These three improvements to an enzymatic incubation may be what is missing for a successful enzymatic glucuronidation procedure. Finally, human liver UGT’s generally contain more isoforms and act on a greater variety of xenobiotics.

CHAPTER 2 – PRODUCTION OF GLUCURONIDES

III. Glucuronidation of Epirubicin

Background

The glucuronidation of epirubicin was performed to provide an anticancer glucuronide suitable for prodrug therapy. The design for the incubation conditions came from the publication identifying the glucuronidation enzyme as UGT2B7 (Innocenti, F., et al.).

Materials and Methods

Materials

Human liver microsomes were obtained from BD Biosciences, UDPGA, Alamethicin, Epirubicin, TRIS hydrochloride and TRIS base were all obtained from SIGMA, and Magnesium chloride from Malinckrodt.

Incubation Conditions for Epirubicin Glucuronide

1.5 milliliter Eppendorf tubes contained 50μL each of, 5mg/ml microsomal protein, 175uM Epirubicin (2% MeOH from the 1mg/ml methanolic stock), 250mM TRIS buffer

at pH=7.4, and 25mm $MgCl_2$. The tubes containing the above ingredients were placed in an ice bath then 20µL of 1mg/ml alamethicin was added as a pore forming antibiotic to increase the bioavailability of UDPGA within the lumen of rectuloendoplasmic folds of the microsomes protein. This pore-forming antibiotic incubation was performed for 30 minutes in an ice bath, before addition of UDPGA to start the reaction. All samples were then removed from the ice bath and placed in a 37°C shaking water bath incubator. After 5 minutes the samples were at 37°C and the glucuronidation reaction was initated by the addition of 50µL of 4mg/ml UDPGA (5mM). After 4 hours of incubation the majority of the epirubicin substrate was converted to its glucuronide at a rate of 5uM/hour.

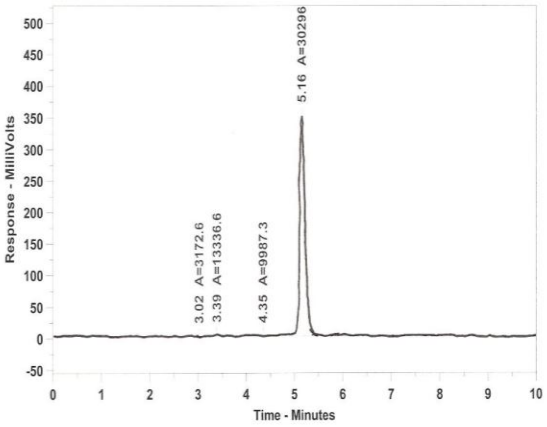

Peak #	Ret. Time	Name	Amount	Amt %	Area	Height
1	3.02		0.00	N/A	3173	427
2	3.39		0.00	N/A	13337	2118
3	4.35		0.00	N/A	9987	1097
4	5.16		0.00	N/A	3029697	349488

Figure 2.7 (Epirubicin Before Microsomal Incubation)

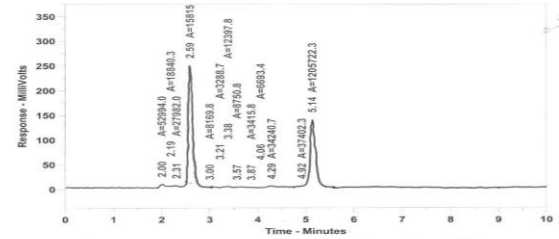

Peak #	Ret. Time	Name	Amount	Amt %	Area	Height
1	2.00		0.00	N/A	52994	7101
2	2.19		0.00	N/A	18840	3029
3	2.31		0.00	N/A	27982	3931
4	2.59		0.00	N/A	1581584	247464
5	3.00		0.00	N/A	8170	1088
6	3.21		0.00	N/A	3289	543
7	3.38		0.00	N/A	12398	1664
8	3.57		0.00	N/A	8751	881
9	3.87		0.00	N/A	3416	491
10	4.06		0.00	N/A	6693	802
11	4.29		0.00	N/A	34241	2977
12	4.92		0.00	N/A	37402	3064
13	5.14		0.00	N/A	1205722	137106

Figure 2.8 (Epirubicin After Microsomal Incubation)

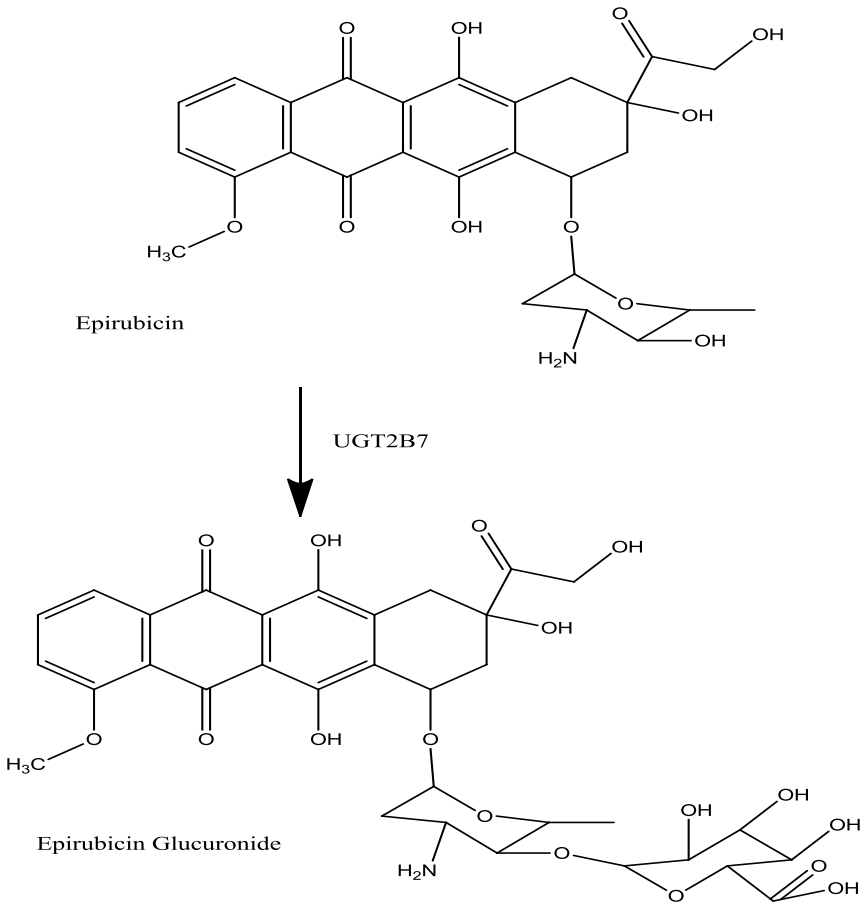

Figure 2.9 (Epirubicin Glucuronide Formation)

250µL of each epirubicin glucuronide containing incubation were loaded into a Millipore Centrifree 30,000 molecular weight cut-off protein filter to remove the microsomal protein and spun at 2000g for 20minutes. Then 200µL of each filtered sample was pipetted into a 1.5ml eppendorf tube and placed in a 37°C shaking water bath for the confirmation and activation experiment.

Confirmation of Epirubicin Glucuronide in-vitro

Conformation of epirubicin glucuronide formation was achieved by incubation with Epirubicin Glucuronide and E.*coli* origin β-glucuronidase. The 200µL filtered samples at 37°C were ready for the hydrolysis confirmation experiment. The hydrolysis of the glucuronide was initiated by the addition of equal volume of glucuronidase (100U/ml) in 4mM phosphate buffer pH=6.8. A time zero sample was taken by the removal of 100µL aliquot of the sample and placing it in 200µL of acetonitrile, vortexing, and placed in the fridge for 30 minutes. Time points at 1.5, 3, and 4 hours were taken the same way. Each sample time point was spun in a centrifuge at 13,000g for 5 minutes. 200µL of the supernatant were added to an autosampler vial and 40µL of each sample were injected onto the HPLC.

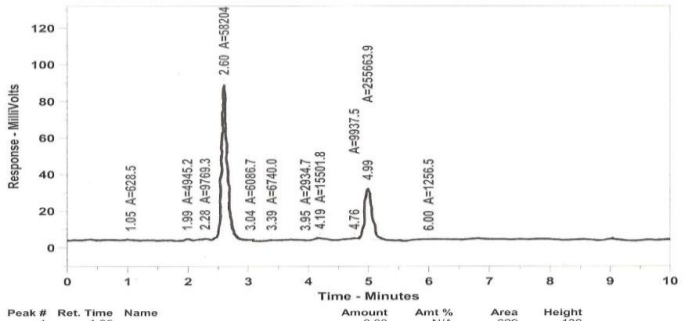

Peak #	Ret. Time	Name	Amount	Amt %	Area	Height
1	1.05		0.00	N/A	629	130
2	1.99		0.00	N/A	4945	572
3	2.28		0.00	N/A	9769	933
4	2.60		0.00	N/A	582049	85392
5	3.04		0.00	N/A	6087	591
6	3.39		0.00	N/A	6740	542
7	3.95		0.00	N/A	2935	346
8	4.19		0.00	N/A	15502	1280
9	4.76		0.00	N/A	9937	1031
10	4.99		0.00	N/A	255664	27917
11	6.00		0.00	N/A	1256	184

Figure 2.10 (Epirubicin Glucuronide Before Glucuronidase Addition)

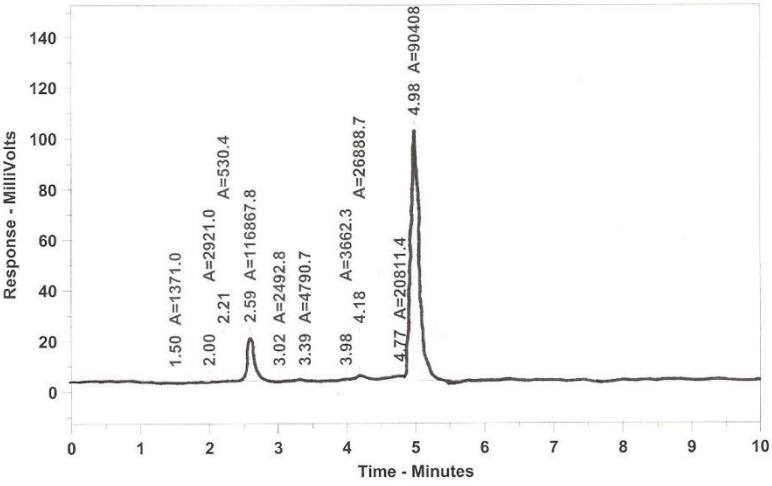

Peak #	Ret. Time	Name	Amount	Amt %	Area	Height
1	1.50		0.00	N/A	1371	189
2	2.00		0.00	N/A	2921	454
3	2.21		0.00	N/A	530	125
4	2.59		0.00	N/A	116868	17443
5	3.02		0.00	N/A	2493	360
6	3.39		0.00	N/A	4791	531
7	3.98		0.00	N/A	3662	496
8	4.18		0.00	N/A	26889	2182
9	4.77		0.00	N/A	20811	1956
10	4.98		0.00	N/A	904086	99120

Figure 2.11 (Epirubicin Glucuronide After Glucuronidase Addition)

HPLC Analytical conditions

Mobile phase consisted of 40% A: 25mM ammonium acetate (1.9g Ammonium Acetate

and 1.2mL Acetic Acid diluted to 1 Liter) and 60% B: Acetonitrile at a flow rate of 1ml/min. The separation was achieved with an Agilent cyano (CN) column 250mm x 4.6mm, 5 micron particle size.

The retention times were 2.59 minutes for the glucuronide and 4.98 minutes for the substrate Epirubicin. The detection was by fluorescence ex=480 and em=560 with a gain of 100 on a Jasco fluorescent HPLC detector.

Results and Discussion

This procedure details the confirmation of the prodrug epirubicin glucuronic acid by the enzyme beta-glucuronidase. Incubation conditions to produce the prodrug were implemented followed by the glucuronidase incubation conditions to revert the prodrug to its aglycone form. The goal of this experiment was to verify a robust assay for measuring the activity of beta glucuronidase-immobilized nanoparticles compared to non-immobilized glucuronidase protein in a rich human biological mimicking enviroment.

The activation of the glucuronide prodrug (epirubicin) was achieved by converting most of the prodrug to the active form within 90 minutes of incubation. Average peak height, for the glucuronide, went from 85,000 millivolts response to 17,000 millivolts by the 90 minute time point.

This assay provided a good test for confirmation of glucuronidase activity but the prodrug concentration is fixed at a starting concentration of 10uM. For further analysis of Epirubicin glucuronide, peaks were collected to produce a pure powder stock of the glucuronide. Collecting the peaks from an HPLC separation and drying under nitrogen provided a concentrate buffered in acetate. This was strong enough for a clean mass spectrum analysis, in an Ion-trap, mass spectrometer, and provided enough concentrated drug for invivo studies.

The mass spectra from the fragmentation of larger ions were used to characterize Epirubicin and Epirubicin glucuronide. The mass data is presented in the subsequent figures.

The fragmentation of these two molecules provided masses of 397.1 and 361.1 that were shared. This further confirmed the production of the prodrug Epirubicin glucuronide. The mass of the epirubicin glucuronide protonated ion was reported to be MW=720.

Figure 2.12 (Epirubicin Fragmentation Pattern)

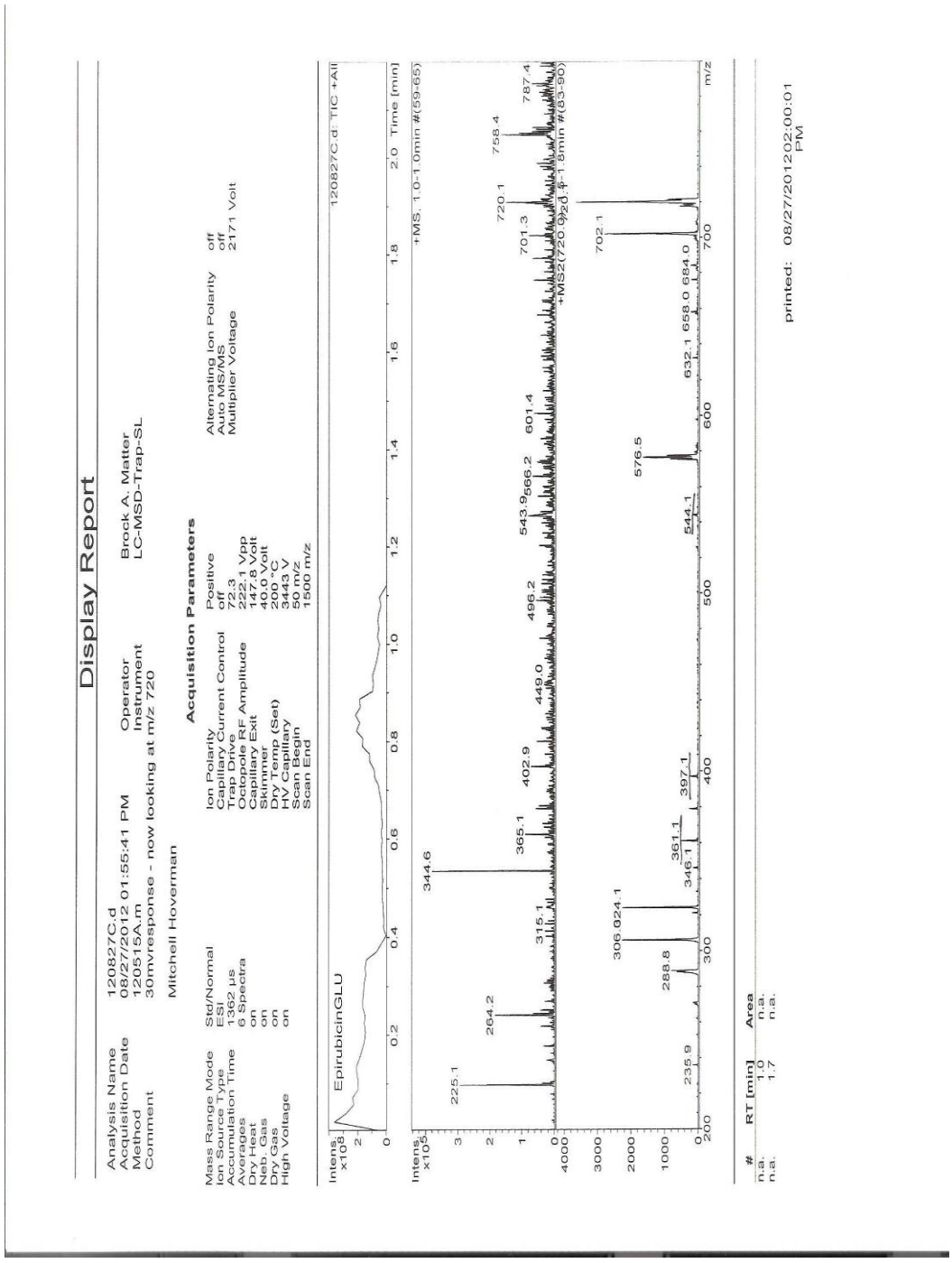

Figure 2.13 (Epirubicin Glucuronide Fragmentation Pattern)

CHAPTER 3: Nanoparticle Production

I: Control of Alginate Nanoparticle Size with Emulsions

Production of Alginate Gel Beads

Background

Alginate Gel Beads were synthesized by dropping an aqueous gel-like mixture containing sodium alginate, β-glucuronidase enzyme, and phosphate buffer (sol mixture), with a hypodermic needle, into a very strong solution of calcium chloride. This was an adaption of a yeast alcohol dehydrogenase immobilization in alginate gel beads procedure that utilized Sodium Alginate, YADH enzyme, and TRIS buffer; as the sol mixture (XU, S., et al. 2006)

One goal was to make the non-micelle micro particles (gel beads) smaller. It was thought that by limiting the flow rate of the alginate enzyme infusion, into the calcium chloride polymerizing solution, with a slowly timed syringe pump; the droplet and resulting particle size would be significantly reduced. This was abandoned when no significant reduction in droplet size was observed. The physical property of producing an aqueous droplet may require formation under a strong vacuum and/or other difficult to replicate conditions, such as those observed during the electrospray ionization of mobile phase in a mass spectrum detector.

The final step was to attach the antibody onto the micelle formed nanoparticle as proof of concept that the alginates' free carboxylate groups on the surface of the particle can be coupled with an antibody. I would do this through the Triazine promoted Amidation of carboxylic acids (Organic process & Development 1999, 3, 172-176 by Rayle and Fellmeth).

Materials and Methods

Materials

Dioctyl sulfosuccinate sodium salt 98%, Sigma (DOSS)

Isopropyl myristate 98%, Sigma (IPM)

Alginic acid sodium salt 20,000-40,000cps viscosity, Sigma

Calcium chloride dihydrate, Merck

Materials Preparation Procedure for Microparticles

A 2% PVA solution was made, by dissolving 1.2g of PVA in 60 ml deionized water. To help dissolve the PVA it was slowly added to the deionized water, in an ice bath, over 30 minutes while stirring. Stirring continued for 2 more hours. Then, the PVA was microwaved for 15 seconds, cooled, and centrifuged at 1000 rpm for 10 minutes to remove the insoluble PVA.

1.5 mL of Alginic Acid Sodium Salt solution were prepared by dissolving 30mg in 1.5 mL of deionized water while stirring for 2 hours. The alginate solution was then sonicated in an ice bath for 5 minutes.

1000U of β-glucuronidase were dissolved in 1.5 mL of deionized water and added to the 1.5 mL alginate solution while stirring for 2 hours, vortex, and sonicated in an ice bath.

6.5 mL of chloroform were used to dissolve 162.5mg of DOSS (2.5% solution).

15 mL of deionized water were used to dissolve 11.9g of calcium chloride dihydrate to produce a 60% calcium solution.

Microparticle Synthesis Procedure

The preparation of a sodium alginate and DOSS (Dioctyl sulfosuccinate sodium salt, 98% Sigma) nanoparticles were produced by forming an emulsion of alginic acid and DOSS which was prepared in 2% polyvinyl alcohol. This emulsion was polymerized with calcium chloride. The particles were then washed three times and purified by centrifugation before freezing and lyophilizing.

1 mL of each alginate solution was placed in a 15 mL tube. To this, 2 mL of the DOSS solution was added. This was vortexed and then sonicated in an ice bath with a sonicator

3000 at level 5 for 5 minutes to form an emulsion.

The samples were poured into 50 mL tubes and 15 mL of the PVA solution were added. The samples were vortexed for 1 minute and then sonicated at level 5 for 5 minutes in an ice bath.

Five ml of the 60% calcium chloride solution were added drop wise, over an hour, while stirring and left to stir overnight.

To remove all traces of solvent the samples were stirred under vacuum for 1 hour in a cupped side arm flask.

Wash and Purification Procedure for Microparticles

The polymerized particles were placed in ultracentrifuge tubes and diluted to a 30ml total volume. These were spun at 35,000xg for 30 minutes. The supernatant was poured off and the particles dispersed in 5ml deionized water by sonication and then diluted to 30mL. This was repeated 3 times.

Removal of the aggregated particles from the nanoparticles was achieved by sonicating the particles then dispersing them in 10 mL of deionized water. The suspension was spun at 1000 rpm for 10 minutes and the supernatant was frozen at -80°C for two hours before lyophilizing for 48 hours.

Solubility Points for Alginate Particles Sized by Emulsions

To find the optimal ratio of a calcium chloride and an alginic acid microemulsion for nanoparticle synthesis, IPM was used in place of PVA (to make the particles smaller or to make the procedure simpler), different concentrations of Alginate were used while keeping the solvent and surfactant concentrations the same.

The general technique utilized was described as a Water-in-Oil nanoemulsion for the preparation of calcium alginate nanoparticles (Machado, A., et al. 2012). This projects modification to this procedure was accomplished with IPM as an enzyme suitable solvent, but still retains the phase inversion temperature emulsification method. The Ostwald ripening phenomenon observed with 0.5%/W aginate compared favorably to peer results and observations (Machado, A. H., D. Lundberg, A. J. Ribeiro, F. J. Veiga, B. Lindman, M. G. Miguel, and U. Olsson. 2012.) A bimodal distribution of nanoparticles was observed to produce a distribution in the sub 1000nm particles size.

Nanoparticle Optimization Procedure

Part1

A 2% w/v solution of alginic acid was prepared in DI water. This was stirred overnight. Fifty μl of this solution were added to 150μL of loading material (phosphate buffer pH=6.8 (4mM) and 1000U of β-glucuronidase) to make a 0.5% alginic solution.

A 0.2M DOSS in IPM solution was made by sonication for 2 hours.

A 60% w/v solution of calcium chloride was prepared with its dihydrate requiring 11.9g/15ml concentration. This was stirred overnight. The solution was diluted to a 0.6% w/v concentration.

One part 0.6% $CaCl_2$ was added to ten parts of the 0.2M DOSS/IPM, to form an emulsion by hand swirling.

The 0.5% alginate solution was added in decreasing concentration by the addition of 20μL of 0.5% algal to 200, 400, 600, 800, or 1000ul increments of the 0.2M DOSS/IPM. At the 20μL/1000ul concentration the algal solution did not crash out and its optimal ratio (maximum solubility) for an emulsion was found.

Part2

Two hundred microliters of the 0.054% $CaCl_2$ micro emulsion were added to 1000μL of the 0.0098% alginic solution.

This mixture was sonicated for 1.5 hours (hand swirling was also sufficient).

This resulted in 1.2ml of a double emulsion ultra-concentrate.

Part 3

Twenty μl of the double emulsion concentrate were added to 10ml of water to form a suspension of 3 layers for the polymerization of nanoparticles by hydrophilic interaction in the aqueous layer. It is presumed the top layer is surfactant, the middle layer is the myristic oil, and the bottom layer is aqueous and rich with nanoparticles.

Results and Discussion

Previously a non-emulsion, a single emulsion with DOSS/chloroform, and a single emulsion technique with DOSS/IPM were used to produce nanoparticles with decreased size (respectively). This time a double emulsion technique was used to reduce the particle size during a hydrophillic polymerization of alginic acid with induced with calcium ions. This technique resulted in 25% 250nm particles and 70% 1 micron particles. The variation in size may be controlled with a syringe pump feeding into the calcium micro emulsion, the use of an ice water bath, and/or sonication during polymerization. This is an improvement over the previous method with the use of isopropyl myristate in place of chloroform, as an emulsion solvent, because the particle sizes were small and the solvent was less likely to denature the enzyme (Nesamony, J., et al.).

This procedure successfully produced nanoparticles through an emulsification. More

diligent washing and a more consistent delivery of the calcium chloride, in the polymerization step, may improve the inconsistency in particle size. By using IPM over PVA the optimal solvent for alginate particle production was found (Nesamony, Shah, Kolling. 2012).

This hydrophilic-induction polymerization procedure was successful and the solubility points for a double emulsion technique were explored. Dynamic light scatter revealed 25% 250nm particles and 70% 1000nm particles. The technique and conditions were improved with this method to provide a smaller, more predictable, particle size.

CHAPTER 3: Nanoparticle Production

II. Mild Condition Protein Embedded Nanoparticle Production

Background

The effect of an ice cold water bath temperature during the polymerization of a calcium chloride and an alginic acid microemulsion for nanoparticle synthesis, with 0.2M DOSS in isopropyl myristate, was successful. So this was done with a high and low concentration of β-glucuronidase. Further preparation of the nanoparticles was done by

centrifuging them at 3381g for 10minutes before measuring them with DLS (Nesamony, J., et al.). This was successful in removing impurities that could be interfering with the DLS measurement.

Previously the double emulsion of calcium chloride and alginic acid was used to produce submicron nanoparticles. In the following procedure; High and low protein particles were made, one with 3.34mg in a 0.5% alginic solution, and another with 0.5mg in a 0.5% alginic solution.

Materials and Methods

Materials

Dioctyl sulfosuccinate sodium salt 98%, Sigma (DOSS)

Isopropyl myristate 98%, Sigma (IPM)

Alginic acid sodium salt 20,000-40,000cps viscosity, Sigma

Calcium chloride dihydrate, Merck

Protein Immobilized Nanoparticles Procedure

Part1 (material prep)

A 2% w/v solution of alginic acid was prepared in DI water. This was stirred overnight. Fifty µl of this were added to 150µL of water containing 3.34mg of protein to make a 0.5% alginic solution (high protein). Low protein particles were created with 0.5mg of protein in a 0.5% alginic solution.

A 0.2M DOSS in IPM solution was made by sonication for 2 hours.

A 60% w/v solution of calcium chloride was prepared with its dihydride requiring 11.9g/15ml concentration. This was stirred overnight. The solution was diluted to a 0.6% w/v concentration.

One part 0.6% $CaCl_2$ was added to ten parts of the 0.2M DOSS/IPM, to form an emulsion by hand swirling, forming a 0.054% $CaCl_2$ micro emulsion.

Part2 (low protein)

1000µL of 2% of the 0.5% alginic solution was prepared by adding 20µL of the 0.5% alginic solution to 1ml of DOSS/IPM. This formed a clear microemulsion.

The 0.054% $CaCl_2$ micro emulsion (200µl) was added to 1000µL of the 0.0098% alginic solution with low protein (0.5mg). This was hand-swirled and resulted in 1.2ml of a double emulsion ultra-concentrate.

The 1.2ml ultra-concentrate was added to a 500ml separation funnel followed by 500ml of ice cold DI water. This was shaken for 30 seconds and kept on ice for one hour. The particles were collected from the bottom layer and refrigerated overnight.

This gave a final calculated concentration of 1μg/ml

Part 3 (high protein)

Two hundred μl of the 0.054% $CaCl_2$ micro emulsion in AOT/IPM were added to 600μL of 0.2M DOSS/IPM comprised of 450μL of 0.2M DOSS/IPM and 150μL 0.5% alginic solution with 2.5mg of protein. This alginic solution was slightly cloudy.

The resulting solution (800μl) containing 2.5mg of protein was added to 6.7ml of ice cold DI water, swirled and placed in an ice bath for one hour, followed by refrigeration.

This gave a final concentration of 0.334 mg/ml of total protein (calculated concentration).

Results and Discussion

1000U (based on phenolphthalein) high enzyme concentration and 150U low enzyme concentration particles were produced. The high protein condition produced 9.5 milligrams of particles. 65% were 27 micrometer particles, 40% were 523 nanometer particles, and 5% were 33 nanometers. The low protein condition produced 14.5 milligrams of particles. 65% were 70 micrometer particles, 4% were 3 micrometer particles, 30% were 277 nanometer particles, and 1% was 31 nanometer particles.

These two methods used an ice bath to control the size of polymerization; coined phase inversion temperature emulsification method (PIT). The high protein conditions formed a

suspension that was shaken just before the addition of water. The low protein conditions produced a clear single twin microemulsion.

Both of these procedures used the Phase Inversion Temperature Method (PIT) to form a suspension of 3 layers for the polymerization of nanoparticles by hydrophilic interaction in the aqueous layer. It is presumed the top layer is surfactant, the middle layer is the myristic oil, and the bottom layer is aqueous and rich with, the highly polar, nanoparticles.

Nanoparticles Images

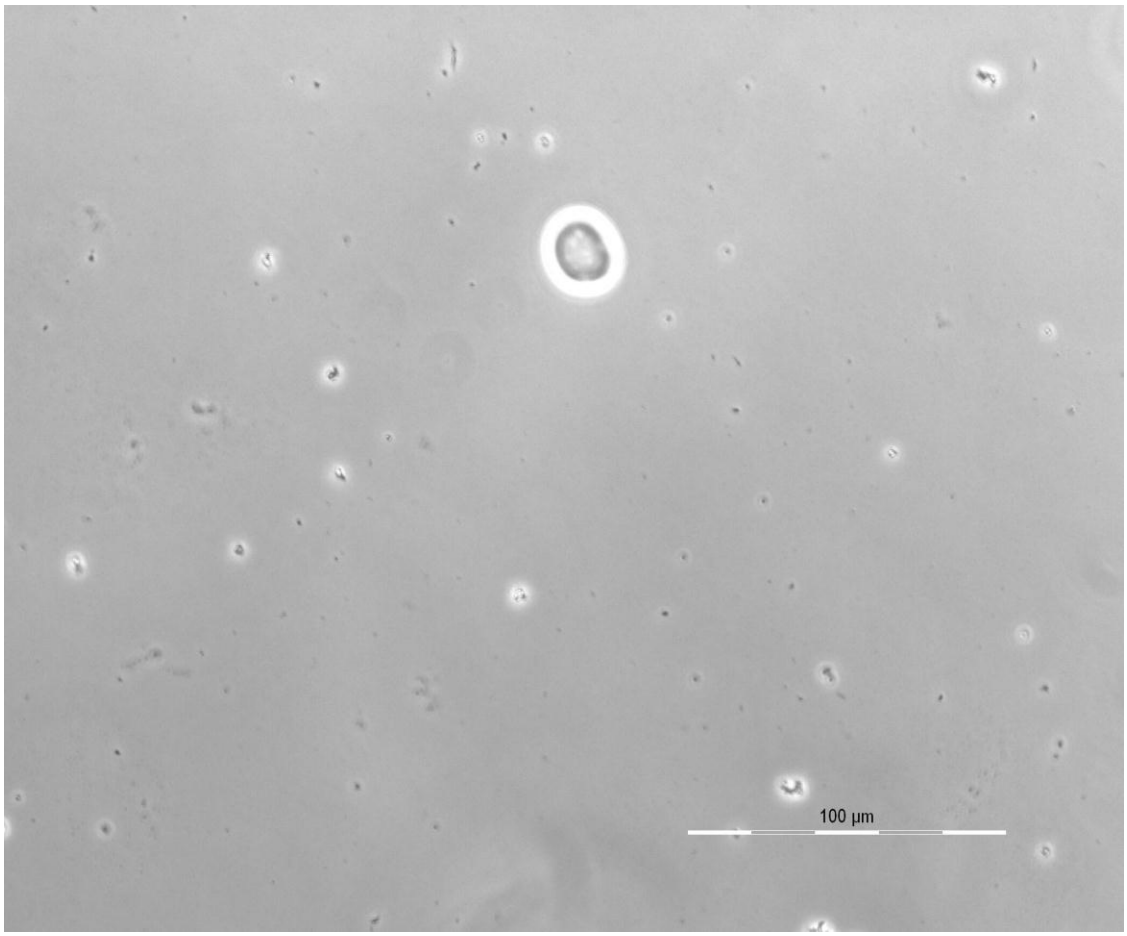

Figure 3.1 (Particles are the Dark Spheres; Oil Droplets are the Light Spheres Image)

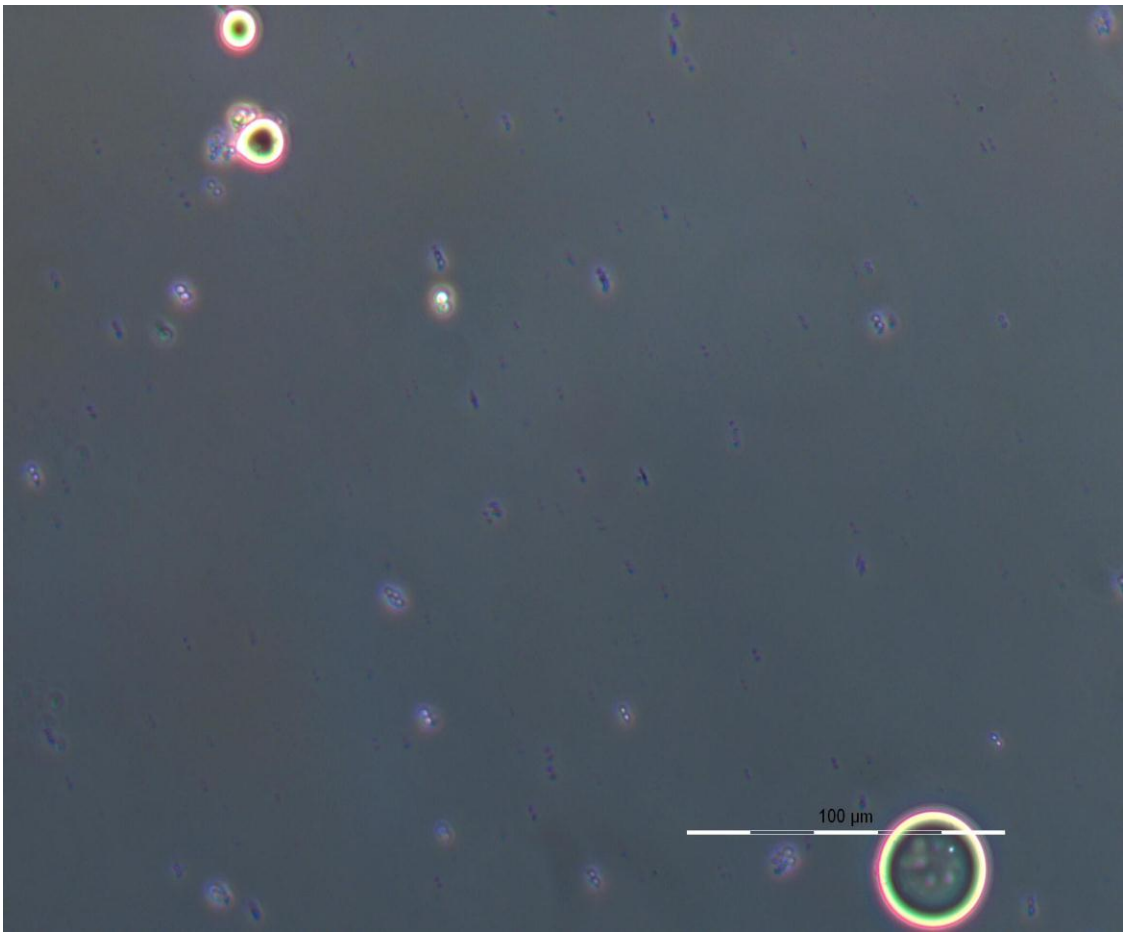

Figure 3.2 (Brownian Motion Movement of Particles Image)

CHAPTER 3: Nanoparticle Production

III. Nanoparticle with Immobilized Protein; Characterization

Background

Beta-glucuronidase is an enzyme capable of cleaving the ester linkage of a glycolsidic bond. The amount of protein was characterized by a reverse biuret method of protein calibration. Two reagents were prepared following the Wang lab SOP. This procedure utilizes albumin as a standard for the calibration curve. The protein was characterized by the loss of absorbance, at 485nm, with increasing protein concentration.

Materials and Methods

Materials

Beta-glucuronidase, bovine serum albumin, copper (II) sulfate pentahydrate, and bathocuproinedisulfonic acid disodium hydrate were purchased from Sigma-Aldrich. potassium sodium-tartrate tetrahydrate and ascorbic acid was purchased from Mallinckrodt. Sodium hydroxide was purchased from Fisher.

Reagents A and B were prepared in in 25mL screw top jars. Reagent A contained: 9.589μL of a $CuSO_4$ (20% w/v) solution, 12.083mg potassium sodium-tartrate

tetrahydrate, 0.48mg NaOH, and de-ionized water to 20mL. Reagent B contained: 5mg ascorbic acid, 7.4mg bathocuproinedisulfonic acid, and de-ionized water to 20mL. The stock reagents were each vortexed and stored at room temperature.

Dioctyl sulfosuccinate sodium salt 98%, Sigma (AOT); Isopropyl myristate 98%, Sigma (IPM); Alginic acid sodium salt 20,000-40,000cps viscosity, Sigma; Calcium chloride dihydrate, Merck; and β-glucuronidase from E.*coli* (1000U/vial), Sigma in 4mM/10ml phosphate buffer

Reverse Biuret Determination of Protein Concentration

Bovine serum albumin was diluted to three concentrations for standard comparison. Concentrations of 1mg/mL, 0.5mg/mL, and 0.1mg/mL were prepared in de-ionized water. A 1000 unit vial of E.*coli* recombinant beta-glucuronidase, containing 4mM phosphate buffer (pH=6.8), was reconstituted with 10mL de-ionized water. The beta-glucuronidase was used as three concentrations. Concentrations of 100%, 50%, and 10% were used as unknowns to be calculated from the albumin standards. 10µL of each of the six aforementioned protein samples were placed into their own 1.5mL reaction cuvette. A zero standard with 10µL of de-ionized water was added to a seventh cuvette. 200µL of

reagent A was added to each of the seven samples. These samples were mixed and incubated at 37°C for five min. Then 1000µL of reagent B were added and incubation continued for 0.5 min. The absorbance, at 485nm, was taken immediately after.

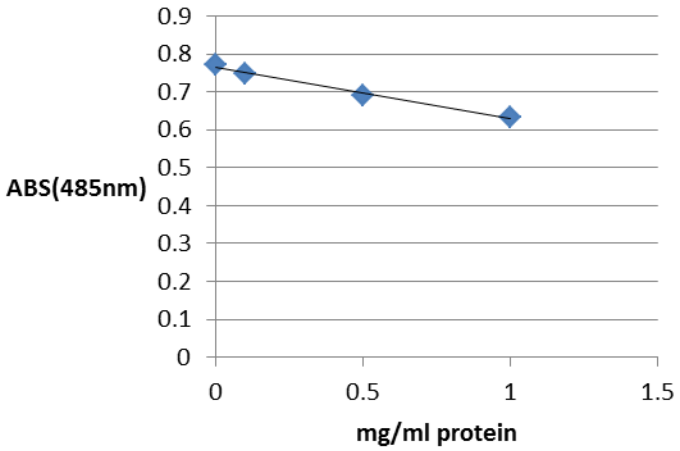

Figure 3.1 (BSA Protein Calibration Chart)

The reduction in absorbance of each sample, at 485nm, had a high correlation with the increase in protein levels of the sample. Figure 3.1 shows a regression coefficient of R^2= 0.99 with the known bovine serum albumin concentrations. The regression analysis produced a linear equation (Y= -0.135x + 0.765) and this was used to determine a 334µg/mL stock concentration of β-Glucuronidase. Given a 10 ml volume, the vial contains 3.34 mg of protein

Table 3.1 Reverse Biuret Method of Protein Determination

ABS(485nM)	Sample	Conc.	Calculated conc.	Zeroed with DI H2O=0.1074	
0.7708	0	blank			
0.6339	1	1mg/ml BSA			
0.69	0.5	0.5mg/ml BSA			
0.7491	0.1	0.1mg/ml BSA		x=(ABS-Yint)/slope	
0.7199	no dilution	10µL B-Gluc	0.334mg/ml	(0.7199-0.765)/-0.135	
0.746	50% of stock	5µL B-Gluc	0.14mg/ml	(0.746-0.765)/-0.135	
0.7688	10% of stock	1µL B-Gluc	0.028mg/mL	0.7688-0.765)/-0.135	

Glucuronidase Loaded Nanoparticles Loading Efficiency

An emulsion (aqueous in oil), described below, was used to produce nanoparticles of 225nm with a SD of 159nm in 90% abundance. β-glucuronidase (2.5mg) was loaded into particles that polymerized in a 7.5ml total volume, yielding a potential of 334μg/ml GUS solution of particles in water. The emulsion (0.5ml) was centrifuged at 9000rpm and supernatant was assayed with equal volume Bradford reagent to show a 7.52μg/ml GUS concentration in the supernatant. The loading efficiency was determined to be 97.75% with a possible 3% variation.

Optimized Method of nanoparticle production with Protein

A 2% w/v solution of alginic acid was prepared in DI water. This was stirred overnight. 50μL of this was added to 150μL of water, containing 3.34mg of protein material, to make a 0.5% alginic solution.

A 0.2M DOSS in IPM solution was made by sonication for 2 hours.

A 60% w/v solution of calcium chloride was prepared with its dihydride requiring

11.9g/15ml concentration. This was stirred overnight. The solution was diluted to a 0.6% w/v concentration.

One part 0.6% $CaCl_2$ was added to ten parts of the 0.2M DOSS/IPM, to form an emulsion by hand swirling, forming a 0.054% $CaCl_2$ micro emulsion.

200μL of the 0.054% $CaCl_2$ micro emulsion in DOSS/IPM were added to 600μL of 0.2M DOSS/IPM comprised of 450μL of 0.2M DOSS/IPM and 150μL 0.5% alginic solution with 2.5mg of protein. This alginic solution was slightly cloudy. (3.34mgx0.75=2.505mg GUS)

The 800μL solution containing 2.5mg of protein was added to 6.7ml of ice cold DI water, swirled and placed in an ice bath for one hour to induce PIT (phase inversion temperatures).

This gave a final concentration of 0.334 mg/ml of total protein calculated concentration (2.505mg/7.5ml total liquid).

A Bradford assay of the nanoparticles supernatant was needed to characterize the loading efficiency was done. This included spinning out the particles at 9000 rpm for 15 minutes and mixing 0.5ml of supernatant with 0.5ml of Bradford reagent at room temp for 10 minutes.

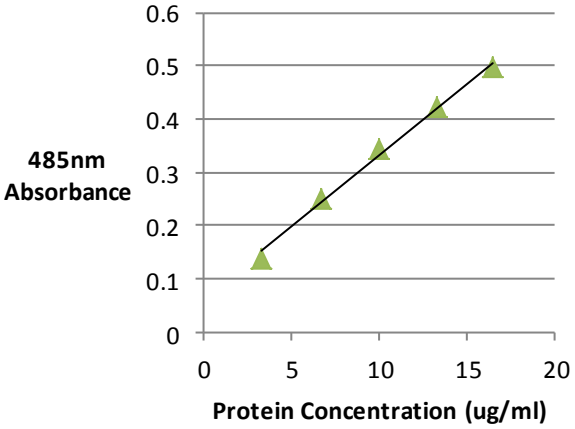

Figure 3.4 (Standard Curve of Protein Concentration)

A standard curve was diluted from a stock of 334µg/ml (previously measured with the biuret assay) down to a range of 16.5µg/ml - 3.34µg/ml.

Results and Discussion

The unknowns and standards were run in triplicate to produce results with less than a 3% coefficient of variation. The regression equation was used to calculate a supernatant concentration of 7.52µg/ml GUS. 7.52488/334= 2.25%. This result was from a final concentration of 0.334 mg/ml of total protein calculated concentration (2.505mg/7.5ml total liquid). The loading efficiency was determined to be 97.75% with a possible 3% variation.

The activity of the particle will need to be tested. Fresh and 2 week old stored particles will be used to cleave p-nitro phenol glucuronide to p-nitro phenol. If this is successful, epirubicin glucuronide will be tested for cleavage and compared to pure GUS stock.

Table 3.2 (Analysis of Variation in Protein Concentration Determination)

Protein Concentration(μg/ml)	16.5	13.36	10.02	6.68	3.34	UKN
485nm Absorbance	0.4813	0.4121	0.3454	0.2496	0.1355	0.2728
485nm Absorbance	0.5057	0.4257	0.3406	0.2513	0.1419	0.2601
485nm Absorbance	0.5010	0.4264	0.3429	0.2497	0.1403	0.2587
Average	0.4960	0.4214	0.3429	0.2502	0.1392	0.2639
SD	0.0129	0.0081	0.0024	0.000954	0.0033	0.0078
CV	2.6100	1.9130	0.6999	0.3813	2.3921	2.9439

CHAPTER 3: Nanoparticle Production

IV: Enzyme Activity of Glucuronidase for Testing Embedded Nanoparticles

Background

This assay resulted in a Vmax of 400umol/mg/min and a Km of 57.68uM. The previous method of producing nanoparticles, by a twin component single emulsion, had a loading efficiency of 97.8%. Next two-week old and freshly-prepared particles will be tested with 4-nitrophenol glucuronide to look for cleavage to 4-nitrophenol. 4-nitrophenol has an absorbance max of 400nm. A spectrophotometric assay can now be employed to compare old and new particles kinetics with the 100U/ml stock solution. This spectrophotometric assay can be compared to the HPLC assay for the accuracy of the method. Upon success, an epirubicin glucuronide cleavage assay will be developed by a HPLC fluorescence method.

Materials and Methods

Materials

β-Glucuronidase, Sigma; 4-Nitrophenyl-glucuronide, SIGMA; 4-Nitrophenol, SIGMA

Methods of Protein Measurement

A max absorbance of 400nm was found for 4-nitrophenol. Concentrations of 100, 50, 25,

15, and 5uM were each used with a 167μg/ml concentration of β-glucuronidase to determine the kinetics for testing the β-glucuronidase embedded nanoparticles. The total volume for the spectrophotometric assay was 1ml by diluting with DI water.

The five concentrations were assayed and so was a standard curve. The slope in the first 30 seconds of the assay was used to calculate the rate of 4-Nitrophenol formation for the 5 concentrations.

Glucuronidase Enzyme Activity after Nanoparticle Synthesis

An optimization of the nanoparticle immobilization procedure was employed and activity was checked to ensure that the nanoparticle forming conditions would not denature the enzyme. There were three particle procedures tried. These procedures were previously described and tested for particle size. These are also provided below. The goal in this round of production was to test for activity with 4-nitrophenyl-glucuronide as an indicator. Only the procedure described below resulted in enzyme activity, although losses in activity were too high and further work must be done to determine how much protein is in the particles and how much is in the surrounding solution.

Method of Activity Detection

A 2% w/v solution of alginic acid was prepared in DI water. This was stirred overnight. This solution was diluted 1:3 to a volume of 200µl and contained 3.34mg of protein material to make a 0.5% alginic solution. These are the "high protein" nanoparticles. Low protein nanoparticles were created with 0.5mg of protein to make a 0.5% alginic solution.

A 0.2M DOSS in IPM solution was made by sonication for 2 hours.

A 60% w/v solution of calcium chloride was prepared with its dihydride requiring 11.9g/15ml concentration. This was stirred overnight. The solution was diluted to a 0.6% w/v concentration.

One part 0.6% $CaCl_2$ was added to ten parts of the 0.2M DOSS/IPM, to form an emulsion by hand swirling, forming a 0.054% $CaCl_2$ micro emulsion.

After materials were prepped, the particle synthesis below was utilized

200µL of the 0.054% $CaCl_2$ micro emulsion in DOSS/IPM were added to 600µL of 0.2M DOSS/IPM comprised of 450µL of 0.2M DOSS/IPM and 150µL 0.5% alginic solution with 2.5mg of protein. This alginic solution was slightly cloudy.

The 800µL solution containing 2.5mg of protein were added to 6.7ml of ice cold DI water, swirled and placed in an ice bath for one hour, followed by refrigeration.

This gave a final concentration of 0.334 mg/ml of total protein calculated concentration.

In this procedure a suspension of 3 layers was formed for the polymerization of nanoparticles by hydrophilic-induction in the aqueous layer. It is presumed the top layer is surfactant, the middle layer is the myristic oil, and the bottom layer is aqueous and rich with nanoparticles.

In order to quantify activity, a max absorbance of 400nm was found for 4-nitrophenol. Concentrations of 100, 50, 25, 15, and 5uM were each used with a 167μg/ml concentration of β-glucuronidase to determine the kinetics for testing the β-glucuronidase embedded nanoparticles. The total volume for the spectrophotometric assay was 1ml by diluting with DI water. The five concentrations were assayed, by spectrophotometry, and a standard curve was made.

Table 3.3 (Activity rates for β-Glucuronidase on 4-Nitrophenol)

substrate conc (μM)	abs	slope	umol change	stdabs	abs is 0.0084x	umols/0.5 min	rate/167μg protein
100	0.76	0.36	42.8	0.7555	0.0063	21.45	128.3
50	0.49	0.26	30.9	0.4859	0.0041	15.5	92.6
25	0.32	0.17	20.1	0.319	0.0027	10.0	60.1
15	0.23	0.12	14.2	0.2305	0.0019	7.12	42.6

5	0.091	0.04	5.27	0.0905	0.0007	2.64	15.8

The activity of the particles, in the three procedures, was assayed and only the ultra-concentrate had any activity at all. In fact, the activity was so high at 20µL/ml of ultra-concentrate the slope was beyond the quantifiable range. Previously, 500µL of a 1000U or 1/20 of the stock was used (167µg protein). For this round, 20µL of a 100µL total volume was used for the assay, after particle production (167x4µg protein). This was to compensate for activity loss.

Results and Discussion

The standard curve was used to convert a change in absorbance into the umol rate of change.

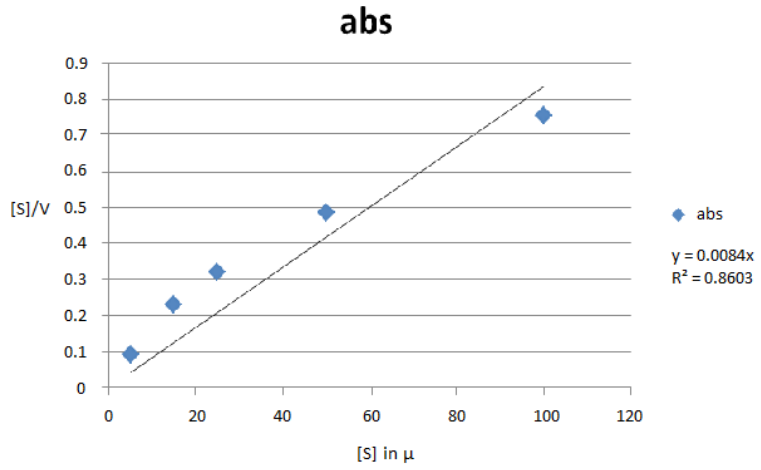

Figure 3.5 (Standard Curve for Micromole Rate of Change)

The Vmax and Km were determined were determined. First, a lineweaver-burke plot was made by ploting the inverse of the rate by the inverse of the substrate concentration.

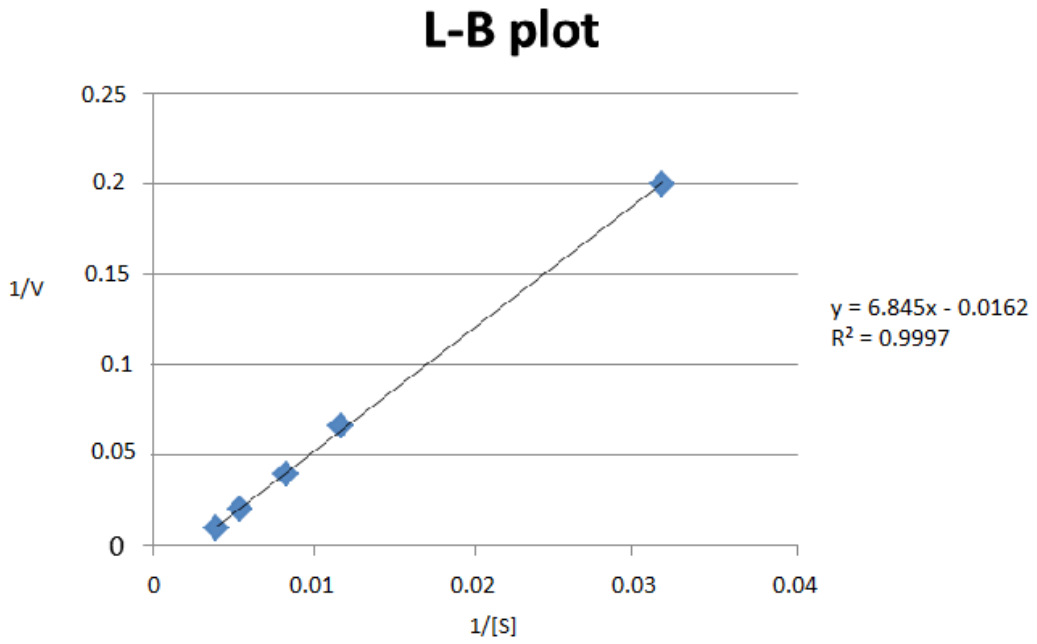

Figure 3.6 (Lineweaver-Burke Plot of Glucuronidase Activity)

This was unsuccessful in determining the kinetics, as shown by the negative intercept. Next a Hanes-Woolf plot was made. These graphs were plotted from the data in the table below.

Table 3.4 (Micromole Change Rate and Substrate Concentration Kinetics)

trial	umolchange rate	substrate conc(uM)	s/v	1/v	1/s
1	256.6	100	0.390	0.00390	0.01
2	185.3	50	0.270	0.00540	0.02
3	120.2	25	0.208	0.00832	0.04
4	85.3	15	0.176	0.0117	0.067
5	31.6	5	0.158	0.0317	0.2

The Woolf plot was plotted using the substrate divided by the rate versus the substrate concentration.

The rates were in umol/mg/min and the Vmax determined was also in micromoles.

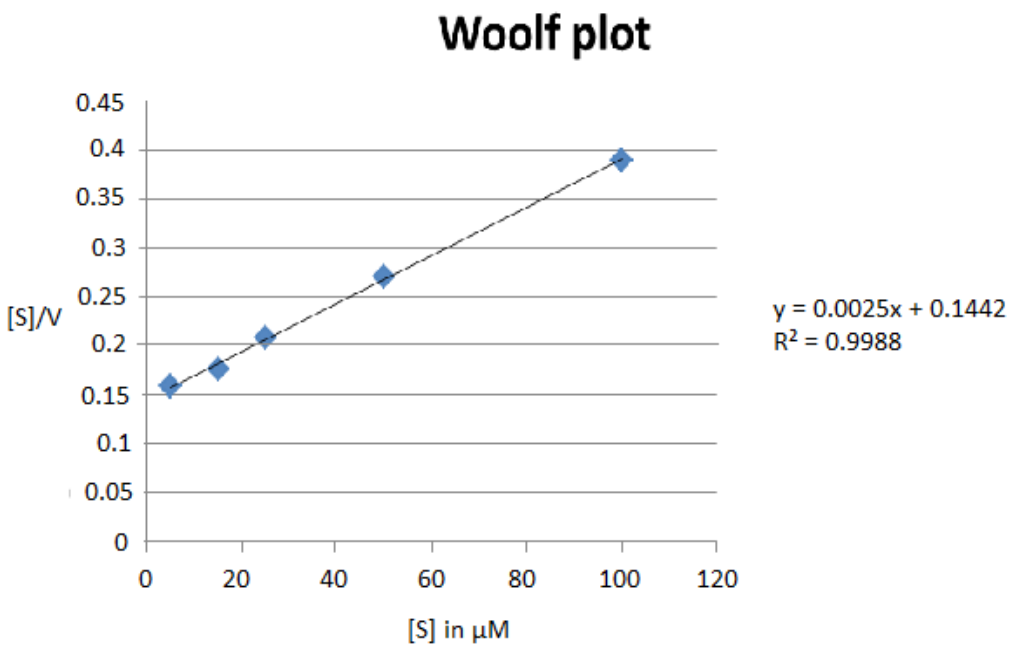

Figure 3.7 (Hanes-Woolf Plot)

In a Woolf plot, the inverse of the slope is the Vmax. So 1/0.0025=400umol/mg/min=Vmax. The intercept is the Km/Vmax=0.1442. When the intercept is multiplied by the Vmax, the Km was obtained.

The Km=57.68uM, this is low compared to the 200uM consensus Km from literature. I would need to use modeling software to get a better approximation, at these low concentrations.

CHAPTER 4: FUTURE DIRECTIONS

Cancer Cell Model for Effectiveness of Prodrug Activating Nanoparticles

To test the effectiveness of this alginate and enzyme complex to target cancer cells, an antibody and cancer cell model would be developed as follows. The Journal of Medicinal Chemistry 2008 article (Lu et al) outlines key integrins for anticancer targets with antibody, peptide, and nonpeptidic inhibitors. Inhibitors can be used to direct the nanoparticle to the target cancer receptor. Receptors are all variants of the vitronectin receptor. The more interesting variants include; AvB3, AvB5, A1B1, A5B1, and A2B1. Start by looking for a cell model that expresses either AvB3 or AvB5. This cell line must also be susceptible to epirubicin, such as breast cancer, GI cancers, or glioma's.

Alternative HHT considerations

An antibody-targeted micro emulsion may be effective in targeted and controlled drug activation with release of HHT. Quick emulsion kits that are designed for antibody conjugated drug delivery are readily available (nofamerica.com sells them). They look very promising and repeatable. Successful delivery has been achieved with taxol-like compounds in micro-emulsions.

Exploration of synthetic glucuronidation routes by addition of glucuronic acid to a side chain precursor for a bio-synthetic scheme or a total organic route of HHT-glucuronide synthesis. This would help characterize the ability of β-glucuronidase from E.*coli* to cleave HHT-glucuronide. Other glucuronides of potent cytotoxins that could be evaluated are daunorubicin glucuronide or SN-38 glucuronide (SN-38 is the active phenolic

metabolite of the anticancer drug irinotecan).

Design of HHT-Glucuronide Total Synthesis

Various attempts to glucuronidate HHT via an enzymatic conjugation with glucuronic acid were unsuccessful. These unsuccessful reactions have led me to try an organic synthesis attempt at conjugating aceto-bromo-glucuronic acid methyl ester and HHT. This reaction only resulted in cleavage of the ester side chain. To further identify the chemical properties of HHT, glucuronidation of the ester side chain of HHT could be attempted. If addition of the protected glucuronic acid on to 6-Hydroxy-6-methyl-2-oxo-heptanoic acid was successful, completion of side chain and addition to the core structure cephalotaxine would follow. If the addition is unsuccessful, it is reasonable to conclude glucuronidation of the HHT side chain may not be possible.

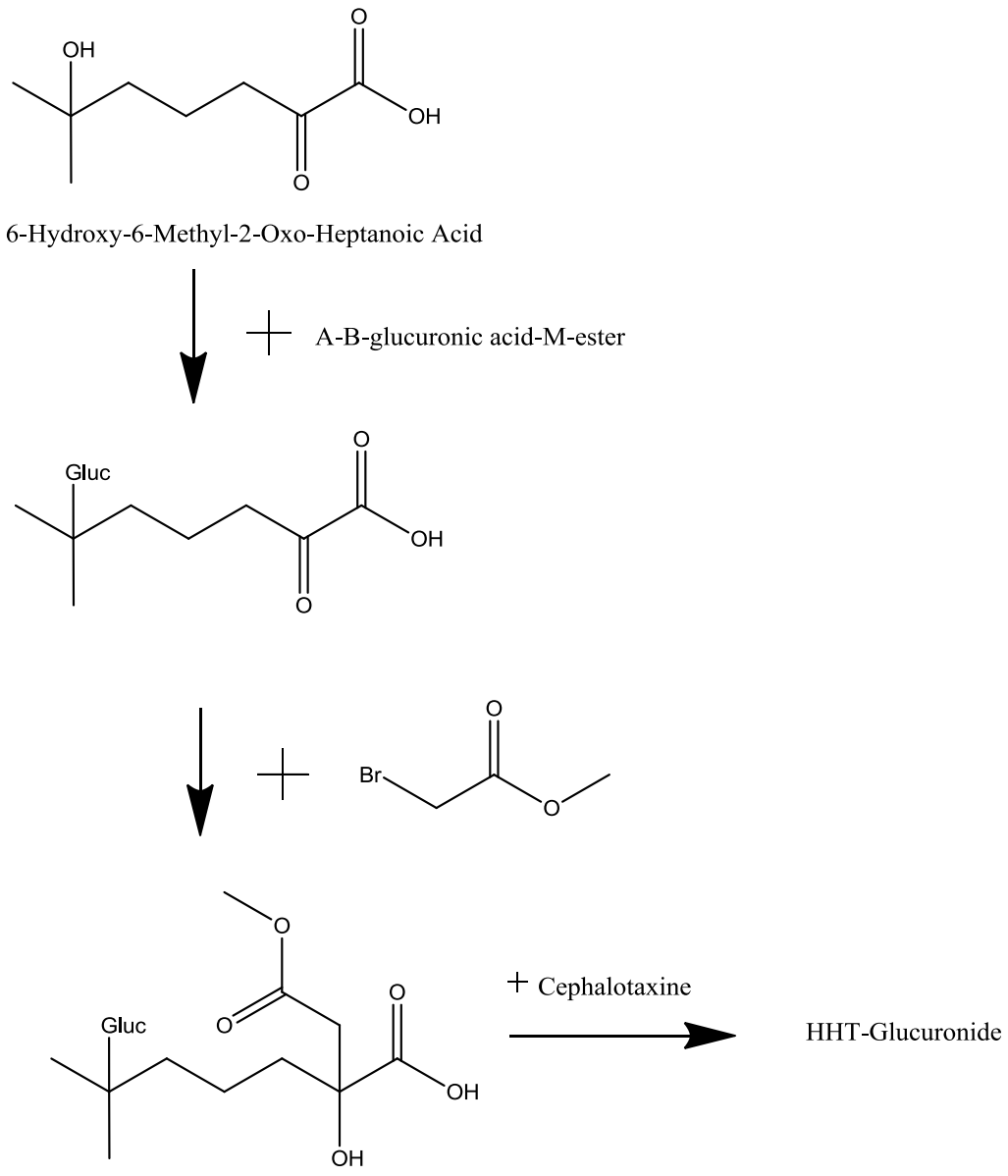

Fig. 4.1 (Reaction Scheme for Organic Synthesis of HHT-Glucuronide)

Method of Production

The first step of the reaction, in the production of a glucuronic acid side chain of HHT, involves the addition of Aceto-Bromo-Glucuronic acid Methyl Ester with 6-Hydroxy-6-methyl-2-Oxo-heptanoic acid. Figure 1.1 shows the overall reaction scheme.

The Method of Production will include a reaction in THF. THF was chosen as a solvent because it is an aprotic solvent that is moderately polar. The reaction will consist of 1 equivalent of the 6-Hydroxy-6-Methyl-2-Oxo-Heptanoic acid dissolved in THF. 2.2 equivalents of lithium hydride base will be added through cannulation under nitrogen. The first proton to be abstracted will be the carboxylate followed by hydroxyl group. This makes the anionic hydroxyl group the most reactive site and the most likely to add the acetyl protected bromo glucuronic acid. One equivalent of acetyl bromo glucuronic acid and silver carbonate or silver triflate catalyst will be dissolved in THF and added to the Heptanoic acid and lithium hydride mixture through cannulation. This, in theory, should facilitate the addition of glucuronic acid to the ester side chain of HHT.

Results and Discussion:

The results could be checked with Negative Electrospray ionization Tandem Mass Spec. This is ideal because of formation of the negative charge on the carboxylate end of the heptanoic acid glucuronate.

The next step involves the addition of the Bromo acetate methyl ester through a Grignard reagent with magnesium catalyst. This would require 6 equivalents of lithium hydride to facilitate site specific addition at the 2 Oxo site of the heptanoic acid. 6 equivalents will be needed to simultaneously cleave the protecting acetyl groups and complete the side chain of HHT.

The procedure is pretty straight forward but the 6-Hydroxy-6-Methyl -2-Oxo-Heptanoic acid needs to be synthesized. Because of the unavailability and difficulty in producing 6-Hydroxy-6-Methyl -2-Oxo-Heptanoic acid, The Synthesis of HHT-Glucuronide was not implemented.

Works Cited

Bibliography (includes non-referenced literature)

Accardo, A., R. Mansi, G. Salzano, A. Morisco, M. Aurilio, A. Parisi, F. Maione, et al. 2012. "Bombesin Peptide Antagonist for Target-Selective Delivery of Liposomal Doxorubicin on Cancer Cells." *Journal of Drug Targeting*. doi:10.3109/1061186X.2012.741138.

Albarghouthi, M., D. A. Fara, M. Saleem, T. El-Thaher, K. Matalka, and A. Badwan. 2000. "Immobilization of Antibodies on Alginate-Chitosan Beads." *International Journal of Pharmaceutics* 206 (1-2): 23-34.

Appel, J. M., B. Zerahn, S. Moller, H. M. Christensen, P. Sogaard, B. Ejlertsen, N. Fogh-Andersen, B. V. Jensen, and D. L. Nielsen. 2012. "Long-Term Heart Function After Adjuvant Epirubicin Chemotherapy for Breast Cancer." *Acta Oncologica (Stockholm, Sweden)* 51 (8): 1054-1061. doi:10.3109/0284186X.2012.702920; 10.3109/0284186X.2012.702920.

Aprile, S., E. Del Grosso, and G. Grosa. 2010. "Identification of the Human UDP-Glucuronosyltransferases Involved in the Glucuronidation of Combretastatin A-4." *Drug Metabolism and Disposition: The Biological Fate of Chemicals* 38 (7): 1141-1146. doi:10.1124/dmd.109.031435.

Aramaki, T., M. Moriguchi, E. Bekku, K. Asakura, A. Sawada, and M. Endo. 2012. "Comparison of Epirubicin Hydrochloride and Miriplatin Hydrate as Anticancer Agents

for Transcatheter Arterial Chemoembolization of Hepatocellular Carcinoma." *Hepatology Research : The Official Journal of the Japan Society of Hepatology*. doi:10.1111/j.1872-034X.2012.01100.x; 10.1111/j.1872-034X.2012.01100.x.

Asano, Y., T. Hiramoto, R. Nishino, Y. Aiba, T. Kimura, K. Yoshihara, Y. Koga, and N. Sudo. 2012. "Critical Role of Gut Microbiota in the Production of Biologically Active, Free Catecholamines in the Gut Lumen of Mice." *American Journal of Physiology.Gastrointestinal and Liver Physiology*. doi:10.1152/ajpgi.00341.2012.

Berman, E. 2011. "Omacetaxine: The FDA Decision." *Clinical Advances in Hematology & Oncology : H&O* 9 (1): 57-58.

Boado, R. J. and W. M. Pardridge. 2010. "Genetic Engineering of IgG-Glucuronidase Fusion Proteins." *Journal of Drug Targeting* 18 (3): 205-211. doi:10.3109/10611860903353362.

Burgess, D. J. and S. Ponsart. 1998. "Beta-Glucuronidase Activity Following Complex Coacervation and Spray Drying Microencapsulation." *Journal of Microencapsulation* 15 (5): 569-579. doi:10.3109/02652049809008241.

Cai, H., C. Ni, and L. Zhang. 2012. "Preparation of Complex Nano-Particles Based on Alginic acid/poly[(2-Dimethylamino) Ethyl Methacrylate] and a Drug Vehicle for Doxorubicin Release Controlled by Ionic Strength." *European Journal of Pharmaceutical Sciences : Official Journal of the European Federation for Pharmaceutical Sciences* 45 (1-2): 43-49. doi:10.1016/j.ejps.2011.10.020.

Cao, G., J. Li, L. Shen, and X. Zhu. 2012. "Transcatheter Arterial Chemoembolization for Gastrointestinal Stromal Tumors with Liver Metastases." *World Journal of Gastroenterology : WJG* 18 (42): 6134-6140. doi:10.3748/wjg.v18.i42.6134; 10.3748/wjg.v18.i42.6134.

Chen, J. K., T. S. Chen, P. Lim, and M. Iqbal. 2012. "Drug-Induced Subacute Cutaneous Lupus Erythematosus Associated with Doxorubicin." *Journal of the American Academy of Dermatology* 67 (6): e273-5. doi:10.1016/j.jaad.2012.05.021; 10.1016/j.jaad.2012.05.021.

Chen, L., B. A. Mooso, M. K. Jathal, A. Madhav, S. D. Johnson, E. van Spyk, M. Mikhailova, et al. 2011. "Dual EGFR/HER2 Inhibition Sensitizes Prostate Cancer Cells to Androgen Withdrawal by Suppressing ErbB3." *Clinical Cancer Research : An Official Journal of the American Association for Cancer Research* 17 (19): 6218-6228. doi:10.1158/1078-0432.CCR-11-1548; 10.1158/1078-0432.CCR-11-1548.

Chen, R., L. Guo, Y. Chen, Y. Jiang, W. G. Wierda, and W. Plunkett. 2011. "Homoharringtonine Reduced Mcl-1 Expression and Induced Apoptosis in Chronic Lymphocytic Leukemia." *Blood* 117 (1): 156-164. doi:10.1182/blood-2010-01-262808.

Chen, Y., C. Peng, C. Sullivan, D. Li, and S. Li. 2010. "Novel Therapeutic Agents Against Cancer Stem Cells of Chronic Myeloid Leukemia." *Anti-Cancer Agents in Medicinal Chemistry* 10 (2): 111-115.

Cheng, C. M., Y. L. Lu, K. H. Chuang, W. C. Hung, J. Shiea, Y. C. Su, C. H. Kao, B. M. Chen, S. Roffler, and T. L. Cheng. 2008. "Tumor-Targeting Prodrug-Activating Bacteria

for Cancer Therapy." *Cancer Gene Therapy* 15 (6): 393-401. doi:10.1038/cgt.2008.10.

Cheng, Y., S. Yu, X. Zhen, X. Wang, W. Wu, and X. Jiang. 2012. "Alginic Acid Nanoparticles Prepared through Counterion Complexation Method as a Drug Delivery System." *ACS Applied Materials & Interfaces* 4 (10): 5325-5332. doi:10.1021/am3012627; 10.1021/am3012627.

Choi, Y. H., K. P. Yoo, and J. Kim. 2003. "HPLC-Electrospray Ionization-MS-MS Analysis of Cephalotaxus Harringtonia Leaves and Enhancement of the Extraction Efficiency of Alkaloids Therein by SFE." *Journal of Chromatographic Science* 41 (2): 67-72.

Cruet-Hennequart, S., A. M. Prendergast, G. Shaw, F. P. Barry, and M. P. Carty. 2012. "Doxorubicin Induces the DNA Damage Response in Cultured Human Mesenchymal Stem Cells." *International Journal of Hematology* 96 (5): 649-656. doi:10.1007/s12185-012-1196-5; 10.1007/s12185-012-1196-5.

Dalvai, M., O. Mondesert, B. Bugler, S. Manenti, B. Ducommun, and C. Dozier. 2012. "Doxorubicin Promotes Transcriptional Upregulation of Cdc25B in Cancer Cells by Releasing Sp1 from the Promoter." *Oncogene*. doi:10.1038/onc.2012.524; 10.1038/onc.2012.524.

de Graaf, M., T. J. Nevalainen, H. W. Scheeren, H. M. Pinedo, H. J. Haisma, and E. Boven. 2004. "A Methylester of the Glucuronide Prodrug DOX-GA3 for Improvement of Tumor-Selective Chemotherapy." *Biochemical Pharmacology* 68 (11): 2273-2281. doi:10.1016/j.bcp.2004.08.004.

de Graaf, M., H. M. Pinedo, D. Oosterhoff, I. H. van der Meulen-Muileman, W. R. Gerritsen, H. J. Haisma, and E. Boven. 2004. "Pronounced Antitumor Efficacy by Extracellular Activation of a Doxorubicin-Glucuronide Prodrug After Adenoviral Vector-Mediated Expression of a Human Antibody-Enzyme Fusion Protein." *Human Gene Therapy* 15 (3): 229-238. doi:10.1089/104303404322886084.

Dessi, M., A. Piras, C. Madeddu, C. Cadeddu, M. Deidda, E. Massa, G. Antoni, G. Mantovani, and G. Mercuro. 2011. "Long-Term Protective Effects of the Angiotensin Receptor Blocker Telmisartan on Epirubicin-Induced Inflammation, Oxidative Stress and Myocardial Dysfunction." *Experimental and Therapeutic Medicine* 2 (5): 1003-1009. doi:10.3892/etm.2011.305.

Earl, H. M., L. Hiller, J. A. Dunn, A. L. Vallier, S. J. Bowden, S. D. Jordan, F. Blows, et al. 2012. "Adjuvant Epirubicin Followed by Cyclophosphamide, Methotrexate and Fluorouracil (CMF) Vs CMF in Early Breast Cancer: Results with Over 7 Years Median Follow-Up from the Randomised Phase III NEAT/BR9601 Trials." *British Journal of Cancer* 107 (8): 1257-1267. doi:10.1038/bjc.2012.370; 10.1038/bjc.2012.370.

Engstrom, E. J. 2006. "Nazi Psychoanalysis." *History of Psychiatry* 17 (66 Pt 2): 237-241.

Engstrom, K. M., J. F. Daanen, S. Wagaw, and A. O. Stewart. 2006. "Gram Scale Synthesis of the Glucuronide Metabolite of ABT-724." *The Journal of Organic Chemistry* 71 (22): 8378-8383. doi:10.1021/jo0611972.

Erickson, H. P. 2009. "Size and Shape of Protein Molecules at the Nanometer Level

Determined by Sedimentation, Gel Filtration, and Electron Microscopy." *Biological Procedures Online* 11: 32-51. doi:10.1007/s12575-009-9008-x; 10.1007/s12575-009-9008-x.

F Antunes, I., H. J. Haisma, P. H. Elsinga, V. Di Gialleonardo, Av Waarde, A. T. Willemsen, R. A. Dierckx, and E. F. de Vries. 2012. "Induction of Beta-Glucuronidase Release by Cytostatic Agents in Small Tumors." *Molecular Pharmaceutics* 9 (11): 3277-3285. doi:10.1021/mp300327w; 10.1021/mp300327w.

Fan, J., S. M. Brown, Z. Tu, and E. D. Kharasch. 2011. "Chemical and Enzyme-Assisted Syntheses of Norbuprenorphine-3-Beta-D-Glucuronide." *Bioconjugate Chemistry* 22 (4): 752-758. doi:10.1021/bc100550u; 10.1021/bc100550u.

Fang, Y. P., P. C. Wu, Y. B. Huang, C. C. Tzeng, Y. L. Chen, Y. H. Hung, M. J. Tsai, and Y. H. Tsai. 2012. "Modification of Polyethylene Glycol Onto Solid Lipid Nanoparticles Encapsulating a Novel Chemotherapeutic Agent (PK-L4) to Enhance Solubility for Injection Delivery." *International Journal of Nanomedicine* 7: 4995-5005. doi:10.2147/IJN.S34301; 10.2147/IJN.S34301.

Fleischer, C. C. and C. K. Payne. 2012. "Nanoparticle Surface Charge Mediates the Cellular Receptors used by Protein-Nanoparticle Complexes." *The Journal of Physical Chemistry.B* 116 (30): 8901-8907. doi:10.1021/jp304630q.

Gan, Z., T. Zhang, Y. Liu, and D. Wu. 2012. "Temperature-Triggered Enzyme Immobilization and Release Based on Cross-Linked Gelatin Nanoparticles." *PloS One* 7 (10): e47154. doi:10.1371/journal.pone.0047154; 10.1371/journal.pone.0047154.

Gao, Y., Y. Chen, X. Ji, X. He, Q. Yin, Z. Zhang, J. Shi, and Y. Li. 2011. "Controlled Intracellular Release of Doxorubicin in Multidrug-Resistant Cancer Cells by Tuning the Shell-Pore Sizes of Mesoporous Silica Nanoparticles." *ACS Nano* 5 (12): 9788-9798. doi:10.1021/nn2033105.

Gieling, R. G., C. A. Parker, L. A. De Costa, N. Robertson, A. L. Harris, I. J. Stratford, and K. J. Williams. 2012. "Inhibition of Carbonic Anhydrase Activity Modifies the Toxicity of Doxorubicin and Melphalan in Tumour Cells in Vitro." *Journal of Enzyme Inhibition and Medicinal Chemistry*. doi:10.3109/14756366.2012.736979.

Gonzales, A. J., K. E. Hook, I. W. Althaus, P. A. Ellis, E. Trachet, A. M. Delaney, P. J. Harvey, et al. 2008. "Antitumor Activity and Pharmacokinetic Properties of PF-00299804, a Second-Generation Irreversible Pan-erbB Receptor Tyrosine Kinase Inhibitor." *Molecular Cancer Therapeutics* 7 (7): 1880-1889. doi:10.1158/1535-7163.MCT-07-2232; 10.1158/1535-7163.MCT-07-2232.

Gu, L. F., W. G. Zhang, F. X. Wang, X. M. Cao, Y. X. Chen, A. L. He, J. Liu, and X. R. Ma. 2011. "Low Dose of Homoharringtonine and Cytarabine Combined with Granulocyte Colony-Stimulating Factor Priming on the Outcome of Relapsed Or Refractory Acute Myeloid Leukemia." *Journal of Cancer Research and Clinical Oncology* 137 (6): 997-1003. doi:10.1007/s00432-010-0947-z.

Haisma, H. J., E. Boven, M. van Muijen, J. de Jong, W. J. van der Vijgh, and H. M. Pinedo. 1992. "A Monoclonal Antibody-Beta-Glucuronidase Conjugate as Activator of the Prodrug Epirubicin-Glucuronide for Specific Treatment of Cancer." *British Journal of*

Cancer 66 (3): 474-478.

Hamon, F., B. Renoux, C. Chadeneau, J. M. Muller, and S. Papot. 2010. "Study of a Cyclopamine Glucuronide Prodrug for the Selective Chemotherapy of Glioblastoma." *European Journal of Medicinal Chemistry* 45 (4): 1678-1682. doi:10.1016/j.ejmech.2009.12.067.

He, Q., L. Wen, Q. Li, J. Xu, and F. Luo. 2007. "Fabrication of Alginate Microsphere for Controlled Release and Investigation of its Release Characteristics in Vitro." *Sheng Wu Yi Xue Gong Cheng Xue Za Zhi = Journal of Biomedical Engineering = Shengwu Yixue Gongchengxue Zazhi* 24 (6): 1301-1304.

Hersey, J. C., J. M. Nonnemaker, and G. Homsi. 2010. "Menthol Cigarettes Contribute to the Appeal and Addiction Potential of Smoking for Youth." *Nicotine & Tobacco Research : Official Journal of the Society for Research on Nicotine and Tobacco* 12 Suppl 2: S136-46. doi:10.1093/ntr/ntq173; 10.1093/ntr/ntq173.

Hersey, P., J. Sosman, S. O'Day, J. Richards, A. Bedikian, R. Gonzalez, W. Sharfman, et al. 2010. "A Randomized Phase 2 Study of Etaracizumab, a Monoclonal Antibody Against Integrin Alpha(v)Beta(3), + Or - Dacarbazine in Patients with Stage IV Metastatic Melanoma." *Cancer* 116 (6): 1526-1534. doi:10.1002/cncr.24821; 10.1002/cncr.24821.

Hillard, C. J., S. Manna, M. J. Greenberg, R. DiCamelli, R. A. Ross, L. A. Stevenson, V. Murphy, R. G. Pertwee, and W. B. Campbell. 1999. "Synthesis and Characterization of Potent and Selective Agonists of the Neuronal Cannabinoid Receptor (CB1)." *The*

Journal of Pharmacology and Experimental Therapeutics 289 (3): 1427-1433.

Hook, D. J., C. F. More, J. J. Yacobucci, G. Dubay, and S. O'Connor. 1987. "Integrated Biological-Physicochemical System for the Identification of Antitumor Compounds in Fermentation Broths." *Journal of Chromatography* 385: 99-108.

Houba, P. H., E. Boven, and H. J. Haisma. 1996. "Improved Characteristics of a Human Beta-Glucuronidase-Antibody Conjugate After Deglycosylation for use in Antibody-Directed Enzyme Prodrug Therapy." *Bioconjugate Chemistry* 7 (5): 606-611. doi:10.1021/bc960055j.

Houba, P. H., R. G. Leenders, E. Boven, J. W. Scheeren, H. M. Pinedo, and H. J. Haisma. 1996. "Characterization of Novel Anthracycline Prodrugs Activated by Human Beta-Glucuronidase for use in Antibody-Directed Enzyme Prodrug Therapy." *Biochemical Pharmacology* 52 (3): 455-463.

Huang, B. T., Q. C. Zeng, J. Yu, X. L. Liu, Z. Xiao, and H. Q. Zhu. 2012. "High-Dose Homoharringtonine Versus Standard-Dose Daunorubicin is Effective and Safe as Induction and Post-Induction Chemotherapy for Elderly Patients with Acute Myeloid Leukemia: A Multicenter Experience from China." *Medical Oncology (Northwood, London, England)* 29 (1): 251-259. doi:10.1007/s12032-011-9820-4.

Innocenti, F., L. Iyer, J. Ramirez, M. D. Green, and M. J. Ratain. 2001. "Epirubicin Glucuronidation is Catalyzed by Human UDP-Glucuronosyltransferase 2B7." *Drug Metabolism and Disposition: The Biological Fate of Chemicals* 29 (5): 686-692.

Jackson, R. C., T. J. Boritzki, P. D. Cook, K. E. Hook, W. R. Leopold, and D. W. Fry. 1989. "Biochemical Pharmacology and Antitumor Properties of 4-Amino-8-[Beta-D-Ribofuranosylamino]Pyrimido-[5,4-d]Pyrimidine." *Advances in Enzyme Regulation* 28: 185-199.

Jain, S. and M. Amiji. 2012. "Tuftsin-Modified Alginate Nanoparticles as a Noncondensing Macrophage-Targeted DNA Delivery System." *Biomacromolecules* 13 (4): 1074-1085. doi:10.1021/bm2017993.

Jathal, M. K., L. Chen, M. Mudryj, and P. M. Ghosh. 2011. "Targeting ErbB3: The New RTK(Id) on the Prostate Cancer Block." *Immunology, Endocrine & Metabolic Agents in Medicinal Chemistry* 11 (2): 131-149. doi:10.2174/187152211795495643.

Ji, J. S., G. J. Teng, H. Y. Yang, J. J. Song, C. Y. Lu, and H. X. Fu. 2012. "Preparation and in Vivo-in Vitro Evaluation of Compond Nanoparticles Loaded with Epirubicin Hydrochloride and Gadopentetate Meglumine." *Zhonghua Yi Xue Za Zhi* 92 (23): 1626-1629.

Jiang, T., Z. Zhang, Y. Zhang, H. Lv, J. Zhou, C. Li, L. Hou, and Q. Zhang. 2012. "Dual-Functional Liposomes Based on pH-Responsive Cell-Penetrating Peptide and Hyaluronic Acid for Tumor-Targeted Anticancer Drug Delivery." *Biomaterials*. doi:10.1016/j.biomaterials.2012.09.027; 10.1016/j.biomaterials.2012.09.027.

Jiang, Z., S. Xu, Y. Lu, W. Yuan, H. Wu, and C. Lv. 2006. "Nanotube-Doped Alginate Gel as a Novel Carrier for BSA Immobilization." *Journal of Biomaterials Science.Polymer Edition* 17 (1-2): 21-35.

Juan, T. Y., S. R. Roffler, H. S. Hou, S. M. Huang, K. C. Chen, Y. L. Leu, Z. M. Prijovich, et al. 2009. "Antiangiogenesis Targeting Tumor Microenvironment Synergizes Glucuronide Prodrug Antitumor Activity." *Clinical Cancer Research : An Official Journal of the American Association for Cancer Research* 15 (14): 4600-4611. doi:10.1158/1078-0432.CCR-09-0090.

Kadam, R. S., D. W. Bourne, and U. B. Kompella. 2012. "Nano-Advantage in Enhanced Drug Delivery with Biodegradable Nanoparticles: Contribution of Reduced Clearance." *Drug Metabolism and Disposition: The Biological Fate of Chemicals* 40 (7): 1380-1388. doi:10.1124/dmd.112.044925.

Kamal, A., V. Tekumalla, P. Raju, V. G. Naidu, P. V. Diwan, and R. Sistla. 2008. "Pyrrolo[2,1-c][1,4]Benzodiazepine-Beta-Glucuronide Prodrugs with a Potential for Selective Therapy of Solid Tumors by PMT and ADEPT Strategies." *Bioorganic & Medicinal Chemistry Letters* 18 (13): 3769-3773. doi:10.1016/j.bmcl.2008.05.038.

Kantarjian, H. M., M. Talpaz, V. Santini, A. Murgo, B. Cheson, and S. M. O'Brien. 2001. "Homoharringtonine: History, Current Research, and Future Direction." *Cancer* 92 (6): 1591-1605.

Karim, H., A. Bogason, H. Bhuiyan, A. K. Fotoohi, P. Lafolie, and S. Vitols. 2012. "Comparison of Uptake Mechanisms for Anthracyclines in Human Leukemic Cells." *Current Drug Delivery*.

Kodiyan, A., E. A. Silva, J. Kim, M. Aizenberg, and D. J. Mooney. 2012. "Surface Modification with Alginate-Derived Polymers for Stable, Protein-Repellent, Long-

Circulating Gold Nanoparticles." *ACS Nano* 6 (6): 4796-4805. doi:10.1021/nn205073n; 10.1021/nn205073n.

Kojima, C., T. Suehiro, K. Watanabe, M. Ogawa, A. Fukuhara, E. Nishisaka, A. Harada, K. Kono, T. Inui, and Y. Magata. 2012. "Doxorubicin-Conjugated Dendrimer/Collagen Hybrid Gels for Metastasis-Associated Drug Delivery System." *Acta Biomaterialia*. doi:10.1016/j.actbio.2012.11.013; 10.1016/j.actbio.2012.11.013.

Kuhn, J., C. Prante, K. Kleesiek, and C. Gotting. 2009. "Measurement of Mycophenolic Acid and its Glucuronide using a Novel Rapid Liquid Chromatography-Electrospray Ionization Tandem Mass Spectrometry Assay." *Clinical Biochemistry* 42 (1-2): 83-90. doi:10.1016/j.clinbiochem.2008.10.004.

Laroui, H., S. V. Sitaraman, and D. Merlin. 2012. "Gastrointestinal Delivery of Anti-Inflammatory Nanoparticles." *Methods in Enzymology* 509: 101-125. doi:10.1016/B978-0-12-391858-1.00006-X.

Lawrentschuk, N., N. Daljeet, C. Ma, K. Hersey, A. Zlotta, and N. Fleshner. 2011. "Prostate-Specific Antigen Test Result Interpretation when Combined with Risk Factors for Recommendation of Biopsy: A Survey of Urologist's Practice Patterns." *International Urology and Nephrology* 43 (1): 31-37. doi:10.1007/s11255-010-9772-1; 10.1007/s11255-010-9772-1.

Lebre, F., D. Bento, S. Jesus, and O. Borges. 2012. "Chitosan-Based Nanoparticles as a Hepatitis B Antigen Delivery System." *Methods in Enzymology* 509: 127-142. doi:10.1016/B978-0-12-391858-1.00007-1.

Legigan, T., J. Clarhaut, B. Renoux, I. Tranoy-Opalinski, A. Monvoisin, J. M. Berjeaud, F. Guilhot, and S. Papot. 2012. "Synthesis and Antitumor Efficacy of a Beta-Glucuronidase-Responsive Albumin-Binding Prodrug of Doxorubicin." *Journal of Medicinal Chemistry* 55 (9): 4516-4520. doi:10.1021/jm300348r.

Legigan, T., J. Clarhaut, I. Tranoy-Opalinski, A. Monvoisin, B. Renoux, M. Thomas, A. Le Pape, S. Lerondel, and S. Papot. 2012. "The First Generation of Beta-Galactosidase-Responsive Prodrugs Designed for the Selective Treatment of Solid Tumors in Prodrug Monotherapy." *Angewandte Chemie (International Ed.in English)* 51 (46): 11606-11610. doi:10.1002/anie.201204935; 10.1002/anie.201204935.

Lertsutthiwong, P. and P. Rojsitthisak. 2011. "Chitosan-Alginate Nanocapsules for Encapsulation of Turmeric Oil." *Die Pharmazie* 66 (12): 911-915.

Leu, Y. L., C. S. Chen, Y. J. Wu, and J. W. Chern. 2008. "Benzyl Ether-Linked Glucuronide Derivative of 10-Hydroxycamptothecin Designed for Selective Camptothecin-Based Anticancer Therapy." *Journal of Medicinal Chemistry* 51 (6): 1740-1746. doi:10.1021/jm701151c.

Levine, A. M., A. Noy, J. Y. Lee, W. Tam, J. C. Ramos, D. H. Henry, S. Parekh, et al. 2012. "Pegylated Liposomal Doxorubicin, Rituximab, Cyclophosphamide, Vincristine, and Prednisone in AIDS-Related Lymphoma: AIDS Malignancy Consortium Study 047." *Journal of Clinical Oncology : Official Journal of the American Society of Clinical Oncology*. doi:10.1200/JCO.2012.42.4648.

Levy, V., S. Zohar, C. Bardin, A. Vekhoff, D. Chaoui, B. Rio, O. Legrand, et al. 2006.

"A Phase I Dose-Finding and Pharmacokinetic Study of Subcutaneous Semisynthetic Homoharringtonine (ssHHT) in Patients with Advanced Acute Myeloid Leukaemia." *British Journal of Cancer* 95 (3): 253-259. doi:10.1038/sj.bjc.6603265.

Li, J., H. Wu, Y. Liang, Z. Jiang, Y. Jiang, and L. Zhang. 2012. "Facile Fabrication of Organic-Inorganic Hybrid Beads by Aminated Alginate Enabled Gelation and Biomimetic Mineralization." *Journal of Biomaterials Science.Polymer Edition*. doi:10.1163/156856212X627351.

Li, Y. F., X. Liu, D. S. Liu, B. H. Din, and J. B. Zhu. 2009. "The Effect of Homoharringtonine in Patients with Chronic Myeloid Leukemia Who have Failed Or Responded Suboptimally to Imatinib Therapy." *Leukemia & Lymphoma* 50 (11): 1889-1891. doi:10.3109/10428190903216838.

Lipshultz, S. E., T. L. Miller, S. R. Lipsitz, D. S. Neuberg, S. E. Dahlberg, S. D. Colan, L. B. Silverman, et al. 2012. "Continuous Versus Bolus Infusion of Doxorubicin in Children with ALL: Long-Term Cardiac Outcomes." *Pediatrics*. doi:10.1542/peds.2012-0727.

Lo, Y. L., C. Y. Hsu, and H. R. Lin. 2012. "PH-and Thermo-Sensitive pluronic/poly(Acrylic Acid) in Situ Hydrogels for Sustained Release of an Anticancer Drug." *Journal of Drug Targeting*. doi:10.3109/1061186X.2012.725406.

Lonning, P. E. and S. Knappskog. 2012. "Chemosensitivity and p53; New Tricks by an Old Dog." *Breast Cancer Research : BCR* 14 (6): 325. doi:10.1186/bcr3326.

Love, S. M., W. Zhang, E. J. Gordon, J. Rao, H. Yang, J. Li, B. Zhang, X. Wang, G. Chen, and B. Zhang. 2012. "A Feasibility Study of the Intraductal Administration of Chemotherapy." *Cancer Prevention Research (Philadelphia, Pa.)*. doi:10.1158/1940-6207.CAPR-12-0228.

Lu, X., D. Lu, M. Scully, and V. Kakkar. 2008. "ADAM Proteins - Therapeutic Potential in Cancer." *Current Cancer Drug Targets* 8 (8): 720-732.

Lu, X., D. Lu, M. F. Scully, and V. V. Kakkar. 2008. "The Role of Integrin-Mediated Cell Adhesion in Atherosclerosis: Pathophysiology and Clinical Opportunities." *Current Pharmaceutical Design* 14 (22): 2140-2158.

Lu, Y. L., X. Q. Yu, Y. Zhu, R. Ba, W. Zhu, and W. R. Xu. 2008. "Expression of Integrins in Bone Marrow Mesenchymal Stem Cells Derived from Patients with Chronic Myeloid Leukemia." *Zhongguo Shi Yan Xue Ye Xue Za Zhi / Zhongguo Bing Li Sheng Li Xue Hui = Journal of Experimental Hematology / Chinese Association of Pathophysiology* 16 (4): 755-758.

Machado, A. H., D. Lundberg, A. J. Ribeiro, F. J. Veiga, B. Lindman, M. G. Miguel, and U. Olsson. 2012. "Preparation of Calcium Alginate Nanoparticles using Water-in-Oil (W/O) Nanoemulsions." *Langmuir : The ACS Journal of Surfaces and Colloids* 28 (9): 4131-4141. doi:10.1021/la204944j.

Mahadeo, K. M. and P. D. Cole. 2010. "Successful Treatment using Omacetaxine for a Patient with CML and BCR-ABL1 [Corrected] 35INS." *Blood* 115 (18): 3852. doi:10.1182/blood-2010-02-269233.

Mahesh, S. 2012. "Ongoing Debate: Anthracyclines and Adjuvant Treatment of Human Epidermal Growth Factor Receptor 2-Positive Breast Cancer." *Journal of Clinical Oncology : Official Journal of the American Society of Clinical Oncology*. doi:10.1200/JCO.2012.44.9991.

Martinez, A., M. Benito-Miguel, I. Iglesias, J. M. Teijon, and M. D. Blanco. 2012. "Tamoxifen-Loaded Thiolated Alginate-Albumin Nanoparticles as Antitumoral Drug Delivery Systems." *Journal of Biomedical Materials Research.Part A* 100 (6): 1467-1476. doi:10.1002/jbm.a.34051; 10.1002/jbm.a.34051.

Martins, S., I. Tho, I. Reimold, G. Fricker, E. Souto, D. Ferreira, and M. Brandl. 2012. "Brain Delivery of Camptothecin by Means of Solid Lipid Nanoparticles: Formulation Design, in Vitro and in Vivo Studies." *International Journal of Pharmaceutics*. doi:10.1016/j.ijpharm.2012.09.054; 10.1016/j.ijpharm.2012.09.054.

Matlow, J. N., K. Aleksa, A. Lubetsky, and G. Koren. 2012. "The Detection and Quantification of Ethyl Glucuronide in Placental Tissue and Placental Perfusate by Headspace Solid-Phase Microextraction Coupled with Gas Chromatography-Mass Spectrometry." *Journal of Population Therapeutics and Clinical Pharmacology = Journal De La Therapeutique Des Populations Et De La Pharamcologie Clinique* 19 (3): e473-82.

Mavinkurve-Groothuis, A. M., K. A. Marcus, M. Pourier, J. Loonen, T. Feuth, P. M. Hoogerbrugge, C. L. de Korte, and L. Kapusta. 2012. "Myocardial 2D Strain Echocardiography and Cardiac Biomarkers in Children during and Shortly After

Anthracycline Therapy for Acute Lymphoblastic Leukaemia (ALL): A Prospective Study." *European Heart Journal Cardiovascular Imaging*. doi:10.1093/ehjci/jes217.

Meng, L., X. Zhang, Q. Lu, Z. Fei, and P. J. Dyson. 2012. "Single Walled Carbon Nanotubes as Drug Delivery Vehicles: Targeting Doxorubicin to Tumors." *Biomaterials* 33 (6): 1689-1698. doi:10.1016/j.biomaterials.2011.11.004.

Meyer-Losic, F., C. Nicolazzi, J. Quinonero, F. Ribes, M. Michel, V. Dubois, C. de Coupade, et al. 2008. "DTS-108, a Novel Peptidic Prodrug of SN38: In Vivo Efficacy and Toxicokinetic Studies." *Clinical Cancer Research : An Official Journal of the American Association for Cancer Research* 14 (7): 2145-2153. doi:10.1158/1078-0432.CCR-07-4580.

Mundra, V., Y. Lu, M. Danquah, W. Li, D. D. Miller, and R. I. Mahato. 2012. "Formulation and Characterization of Polyester/Polycarbonate Nanoparticles for Delivery of a Novel Microtubule Destabilizing Agent." *Pharmaceutical Research*. doi:10.1007/s11095-012-0881-7.

Nesamony, J., P. R. Singh, S. E. Nada, Z. A. Shah, and W. M. Kolling. 2012. "Calcium Alginate Nanoparticles Synthesized through a Novel Interfacial Cross-Linking Method as a Potential Protein Drug Delivery System." *Journal of Pharmaceutical Sciences* 101 (6): 2177-2184. doi:10.1002/jps.23104; 10.1002/jps.23104.

Nesamony, J., C. L. Zachar, R. Jung, F. E. Williams, and S. Nauli. 2012. "Preparation, Characterization, Sterility Validation, and in Vitro Cell Toxicity Studies of Microemulsions Possessing Potential Parenteral Applications." *Drug Development and*

Industrial Pharmacy. doi:10.3109/03639045.2012.671830.

Obradovic, B., J. Stojkovska, Z. Jovanovic, and V. Miskovic-Stankovic. 2012. "Novel Alginate Based Nanocomposite Hydrogels with Incorporated Silver Nanoparticles." *Journal of Materials Science.Materials in Medicine* 23 (1): 99-107. doi:10.1007/s10856-011-4522-1.

Oda, N., K. Shimazu, Y. Naoi, K. Morimoto, A. Shimomura, M. Shimoda, N. Kagara, N. Maruyama, S. J. Kim, and S. Noguchi. 2012. "Intratumoral Regulatory T Cells as an Independent Predictive Factor for Pathological Complete Response to Neoadjuvant Paclitaxel Followed by 5-FU/epirubicin/cyclophosphamide in Breast Cancer Patients." *Breast Cancer Research and Treatment* 136 (1): 107-116. doi:10.1007/s10549-012-2245-8; 10.1007/s10549-012-2245-8.

O'Day, S., A. Pavlick, C. Loquai, D. Lawson, R. Gutzmer, J. Richards, D. Schadendorf, et al. 2011. "A Randomised, Phase II Study of Intetumumab, an Anti-Alphav-Integrin mAb, Alone and with Dacarbazine in Stage IV Melanoma." *British Journal of Cancer* 105 (3): 346-352. doi:10.1038/bjc.2011.183; 10.1038/bjc.2011.183.

Papageorgiou, S. K., F. K. Katsaros, E. P. Favvas, G. E. Romanos, C. P. Athanasekou, K. G. Beltsios, O. I. Tzialla, and P. Falaras. 2012. "Alginate Fibers as Photocatalyst Immobilizing Agents Applied in Hybrid photocatalytic/ultrafiltration Water Treatment Processes." *Water Research* 46 (6): 1858-1872. doi:10.1016/j.watres.2012.01.005.

Rae, J. M., C. J. Creighton, J. M. Meck, B. R. Haddad, and M. D. Johnson. 2007. "MDA-MB-435 Cells are Derived from M14 Melanoma Cells--a Loss for Breast Cancer, but a

Boon for Melanoma Research." *Breast Cancer Research and Treatment* 104 (1): 13-19. doi:10.1007/s10549-006-9392-8.

Reid, J. M., M. J. Kuffel, J. K. Miller, R. Rios, and M. M. Ames. 1999. "Metabolic Activation of Dacarbazine by Human Cytochromes P450: The Role of CYP1A1, CYP1A2, and CYP2E1." *Clinical Cancer Research : An Official Journal of the American Association for Cancer Research* 5 (8): 2192-2197.

Rooseboom, M., J. N. Commandeur, and N. P. Vermeulen. 2004. "Enzyme-Catalyzed Activation of Anticancer Prodrugs." *Pharmacological Reviews* 56 (1): 53-102. doi:10.1124/pr.56.1.3.

Sachidanandam, K., A. A. Gayle, H. I. Robins, and J. M. Kolesar. 2012. "Unexpected Doxorubicin-Mediated Cardiotoxicity in Sisters: Possible Role of Polymorphisms in Histamine n-Methyl Transferase." *Journal of Oncology Pharmacy Practice : Official Publication of the International Society of Oncology Pharmacy Practitioners*. doi:10.1177/1078155212461022.

Saito, Y., K. Sai, K. Maekawa, N. Kaniwa, K. Shirao, T. Hamaguchi, N. Yamamoto, et al. 2009. "Close Association of UGT1A9 IVS1+399C>T with UGT1A1*28, *6, Or *60 Haplotype and its Apparent Influence on 7-Ethyl-10-Hydroxycamptothecin (SN-38) Glucuronidation in Japanese." *Drug Metabolism and Disposition: The Biological Fate of Chemicals* 37 (2): 272-276. doi:10.1124/dmd.108.024208.

Satishkumar, R. and A. Vertegel. 2008. "Charge-Directed Targeting of Antimicrobial Protein-Nanoparticle Conjugates." *Biotechnology and Bioengineering* 100 (3): 403-412.

doi:10.1002/bit.21782.

Shorter, T. N. and T. O'Day. 2011. "Concealed Carry: Best Practices After November 1, 2011." *WMJ : Official Publication of the State Medical Society of Wisconsin* 110 (6): 297-298.

Sideras, K., A. C. Dueck, T. J. Hobday, K. M. Rowland Jr, J. B. Allred, D. W. Northfelt, W. L. Lingle, et al. 2012. "North Central Cancer Treatment Group (NCCTG) N0537: Phase II Trial of VEGF-Trap in Patients with Metastatic Breast Cancer Previously Treated with an Anthracycline and/or a Taxane." *Clinical Breast Cancer* 12 (6): 387-391. doi:10.1016/j.clbc.2012.09.007; 10.1016/j.clbc.2012.09.007.

Tacyildiz, N., D. Ozyoruk, G. Ozelci Kavas, G. Yavuz, E. Unal, H. Dincaslan, S. Atalay, et al. 2012. "Selenium in the Prevention of Anthracycline-Induced Cardiac Toxicity in Children with Cancer." *Journal of Oncology* 2012: 651630. doi:10.1155/2012/651630; 10.1155/2012/651630.

Tan, G., Z. Lou, W. Liao, Z. Zhu, X. Dong, W. Zhang, W. Li, and Y. Chai. 2011. "Potential Biomarkers in Mouse Myocardium of Doxorubicin-Induced Cardiomyopathy: A Metabonomic Method and its Application." *PloS One* 6 (11): e27683. doi:10.1371/journal.pone.0027683.

Thomas, M., J. Clarhaut, I. Tranoy-Opalinski, J. P. Gesson, J. Roche, and S. Papot. 2008. "Synthesis and Biological Evaluation of Glucuronide Prodrugs of the Histone Deacetylase Inhibitor CI-994 for Application in Selective Cancer Chemotherapy." *Bioorganic & Medicinal Chemistry* 16 (17): 8109-8116. doi:10.1016/j.bmc.2008.07.048.

Tian, Q., X. H. Wang, W. Wang, C. N. Zhang, P. Wang, and Z. Yuan. 2012. "Self-Assembly and Liver Targeting of Sulfated Chitosan Nanoparticles Functionalized with Glycyrrhetinic Acid." *Nanomedicine : Nanotechnology, Biology, and Medicine* 8 (6): 870-879. doi:10.1016/j.nano.2011.11.002.

Tietze, L. F., H. J. Schuster, K. Schmuck, I. Schuberth, and F. Alves. 2008. "Duocarmycin-Based Prodrugs for Cancer Prodrug Monotherapy." *Bioorganic & Medicinal Chemistry* 16 (12): 6312-6318. doi:10.1016/j.bmc.2008.05.009.

Toggweiler, S., Y. Odermatt, A. Brauchlin, T. Zander, A. Muller, M. Zuber, R. Winterhalder, and P. Erne. 2012. "The Clinical Value of Echocardiography and Acoustic Cardiography to Monitor Patients Undergoing Anthracycline Chemotherapy." *Clinical Cardiology*. doi:10.1002/clc.22074; 10.1002/clc.22074.

Tracy, T. S. and M. A. Hummel. 2004. "Modeling Kinetic Data from in Vitro Drug Metabolism Enzyme Experiments." *Drug Metabolism Reviews* 36 (2): 231-242. doi:10.1081/DMR-120033999.

Vekariya, K. K., J. Kaur, and K. Tikoo. 2012. "ERalpha Signaling Imparts Chemotherapeutic Selectivity to Selenium Nanoparticles in Breast Cancer." *Nanomedicine : Nanotechnology, Biology, and Medicine* 8 (7): 1125-1132. doi:10.1016/j.nano.2011.12.003; 10.1016/j.nano.2011.12.003.

Wachter, D. L., P. A. Fasching, L. Haeberle, R. Schulz-Wendtland, A. Dimmler, T. Koscheck, S. P. Renner, et al. 2012. "Prognostic Molecular Markers and Neoadjuvant Therapy Response in Anthracycline-Treated Breast Cancer Patients." *Archives of*

Gynecology and Obstetrics. doi:10.1007/s00404-012-2534-9.

Wang, T., Z. Feng, N. He, Z. Wang, S. Li, Y. Guo, and L. Xu. 2007. "A Novel Preparation of Nanocapsules from Alginate-Oligochitosan." *Journal of Nanoscience and Nanotechnology* 7 (12): 4571-4574.

Wang, X., R. Wang, Y. Zhang, C. Liang, H. Ye, F. Cao, and Y. Rao. 2012. "Extending the Detection Window of Diazepam by Directly Analyzing its Glucuronide Metabolites in Human Urine using Liquid Chromatography-Tandem Mass Spectrometry." *Journal of Chromatography.A* 1268: 29-34. doi:10.1016/j.chroma.2012.10.012; 10.1016/j.chroma.2012.10.012.

Westman, E. L., M. J. Canova, I. J. Radhi, K. Koteva, I. Kireeva, N. Waglechner, and G. D. Wright. 2012. "Bacterial Inactivation of the Anticancer Drug Doxorubicin." *Chemistry & Biology* 19 (10): 1255-1264. doi:10.1016/j.chembiol.2012.08.011; 10.1016/j.chembiol.2012.08.011.

Wetzler, M. and D. Segal. 2011. "Omacetaxine as an Anticancer Therapeutic: What is Old is New again." *Current Pharmaceutical Design* 17 (1): 59-64.

Woitiski, C. B., R. J. Neufeld, A. F. Soares, I. V. Figueiredo, F. J. Veiga, and R. A. Carvalho. 2012. "Evaluation of Hepatic Glucose Metabolism Via Gluconeogenesis and Glycogenolysis After Oral Administration of Insulin Nanoparticles." *Drug Development and Industrial Pharmacy* 38 (12): 1441-1450. doi:10.3109/03639045.2011.653789; 10.3109/03639045.2011.653789.

Xu, S. W., Y. Lu, J. Li, Y. F. Zhang, and Z. Y. Jiang. 2007. "Preparation of Novel Silica-Coated Alginate Gel Beads for Efficient Encapsulation of Yeast Alcohol Dehydrogenase." *Journal of Biomaterials Science.Polymer Edition* 18 (1): 71-80.

Xu, W. L., J. Jin, and W. B. Qian. 2010. "Homoharringtonine in Combination with Cytarabine and Aclarubicin as Induction Therapy Improves Remission and Survival of Patients with Higher Risk Myelodysplastic Syndromes." *Chinese Medical Journal* 123 (1): 108-110.

Xu, Y., H. Wang, S. Zhou, M. Yu, X. Wang, K. Fu, Z. Qian, et al. 2012. "Risk of Second Malignant Neoplasms After Cyclophosphamide-Based Chemotherapy with Or without Radiotherapy for Non-Hodgkin Lymphoma." *Leukemia & Lymphoma*. doi:10.3109/10428194.2012.743657.

Xu, Y., C. Zhan, L. Fan, L. Wang, and H. Zheng. 2007. "Preparation of Dual Crosslinked Alginate-Chitosan Blend Gel Beads and in Vitro Controlled Release in Oral Site-Specific Drug Delivery System." *International Journal of Pharmaceutics* 336 (2): 329-337. doi:10.1016/j.ijpharm.2006.12.019.

Yang, Q., X. D. Wang, J. Chen, C. X. Tian, H. J. Li, Y. J. Chen, and Q. Lv. 2012. "A Clinical Study on Regional Lymphatic Chemotherapy using an Activated Carbon Nanoparticle-Epirubicin in Patients with Breast Cancer." *Tumour Biology : The Journal of the International Society for Oncodevelopmental Biology and Medicine* 33 (6): 2341-2348. doi:10.1007/s13277-012-0496-y; 10.1007/s13277-012-0496-y.

Ye, W. L., Z. H. Teng, D. Z. Liu, H. Cui, M. Liu, Y. Cheng, T. H. Yang, Q. B. Mei, and

S. Y. Zhou. 2012. "Synthesis of a New pH-Sensitive Folate-Doxorubicin Conjugate and its Antitumor Activity in Vitro." *Journal of Pharmaceutical Sciences*. doi:10.1002/jps.23381; 10.1002/jps.23381.

Yin, S., R. Wang, F. Zhou, H. Zhang, and Y. Jing. 2011. "Bcl-xL is a Dominant Antiapoptotic Protein that Inhibits Homoharringtonine-Induced Apoptosis in Leukemia Cells." *Molecular Pharmacology* 79 (6): 1072-1083. doi:10.1124/mol.110.068528.

Yu, X. L., Y. Liu, J. D. Wang, D. X. Kong, and C. Y. Chen. 2009. "Changes of Gene Expression Profile in Homoharringtonine-Induced Leukemia Multi-Drug Resistant Cell Line K562/HHT." *Zhonghua Xue Ye Xue Za Zhi = Zhonghua Xueyexue Zazhi* 30 (6): 363-367.

Yuan, P., B. H. Xu, J. Y. Wang, F. Ma, Q. Li, P. Zhang, Y. Fan, Q. Li, and W. M. Wang. 2012. "Docetaxel Plus Carboplatin Versus EC-T as Adjuvant Chemotherapy for Triple-Negative Breast Cancer: Safety Data from a Phase III Randomized Open-Label Trial." *Zhonghua Zhong Liu Za Zhi [Chinese Journal of Oncology]* 34 (6): 465-468.

Zhang, C., Y. Wu, T. Liu, Y. Zhao, X. Wang, W. Wang, and Z. Yuan. 2011. "Antitumor Activity of Drug Loaded Glycyrrhetinic Acid Modified Alginate Nanoparticles on Mice Bearing Orthotopic Liver Tumor." *Journal of Controlled Release : Official Journal of the Controlled Release Society* 152 Suppl 1: e111-3. doi:10.1016/j.jconrel.2011.08.158.

Zhang, H., A. Zhang, C. Guo, C. Shi, Y. Zhang, Q. Liu, A. Sparatore, and C. Wang. 2011. "S-Diclofenac Protects Against Doxorubicin-Induced Cardiomyopathy in Mice Via Ameliorating Cardiac Gap Junction Remodeling." *PloS One* 6 (10): e26441.

doi:10.1371/journal.pone.0026441.

Zhang, Q., J. Tong, H. Chen, L. Jiang, H. Zhu, X. Zhu, H. Yu, J. Liu, and B. Liu. 2012. "A Novel Magnetic Nanoparticle Hyperthermia Combined with ACMF-Dependant Drug Release by DAMMs Injection in VX-2 Liver Tumors." *Journal of Nanoscience and Nanotechnology* 12 (1): 127-131.

Zhao, X., J. Zhang, N. Tong, X. Liao, E. Wang, Z. Li, Y. Luo, and H. Zuo. 2011. "Berberine Attenuates Doxorubicin-Induced Cardiotoxicity in Mice." *The Journal of International Medical Research* 39 (5): 1720-1727.

Zhou, J. Z., X. Kou, and D. Stevenson. 1999. "Rapid Extraction and High-Performance Liquid Chromatographic Determination of Parthenolide in Feverfew (Tanacetum Parthenium)." *Journal of Agricultural and Food Chemistry* 47 (3): 1018-1022.